Monkey dorsolateral prefrontal cortex shows anatomically and functionally specific responses to sequential but not temporal or image changes

Nadira Yusif Rodriguez[1], Aarit Ahuja[1], Debaleena Basu[1,2], and Theresa M. Desrochers*[1,3,4]

1. Department of Neuroscience, Brown University
2. Department of Biosciences and Bioengineering, IIT Bombay, Mumbai, Maharashtra, India
3. Department of Psychiatry and Human Behavior, Brown University
4. Robert J. and Nancy D. Carney Institute for Brain Sciences, Brown University

*Correspondence should be addressed to:

Theresa Desrochers

185 Meeting Street

Providence, RI 02912

Box GL-N

(401) 863-7126

theresa_desrochers@brown.edu

Keywords: nonhuman primate, fMRI, prefrontal cortex, abstract sequence, ramping activation

Acknowledgements

This study was supported by the National Science Foundation (NSF) Established Program to Stimulate Competitive Research (EPSCoR) Neural Basis of Attention Grant 1632738 (N.Y.R. and T.M.D.), the National Institute of General Medical Sciences (NIGMS)-National Institutes of Health (NIH) Initiative to Maximize Student Development Grant IMSD R25GM083270 (N.Y.R.), the NIH-NIGMS Grant COBRE P20GM103645 (T.M.D), NIH National Institutes of Mental Health (NIMH) R21MH125010 (T.M.D.), NSF Faculty Early Career Development (CAREER) Program Award BCS-2143656 (T.M.D.), NMIH Research Project Grant R01MH131615 (T.M.D.), and the Carney Institute for Brain Science Innovation Award (T.M.D.). Part of this research was conducted using computational resources and services at the Center for Computation and Visualization, Brown University (NIH Grant S10OD025181).

We thank Matthew Maestri for his assistance with animal training and data collection. We thank Dr. Michael Worden, Lynn Fanella, Fabienne McEleney, and Brown University's MRI Facilities staff for their support and guidance throughout this project. We thank Dr. Lucija Jankovic-Rapan, Dr. Nicola Palomero-Gallagher and Dr. Seán Froudist-Walsh for their assistance and sharing of the MEBRAINS atlas and regions of interest used for analysis. We also thank Dr. David Sheinberg, Dr. Amitai Shenhav, Dr. Katherine Conen, and Hannah Doyle for their continued support throughout this project and preparation of this publication as well as members of both the Sheinberg and the Desrochers Labs for many helpful discussions and contributions.

Author Contributions

Nadira Yusif Rodriguez: Conceptualization, Investigation, Formal analysis, Writing - Original Draft, Writing - Review & Editing, Visualization. Aarit Ahuja: Investigation, Writing - Review & Editing. Debaleena Basu: Conceptualization, Investigation, Writing - Review & Editing. Theresa M. Desrochers: Conceptualization, Methodology, Investigation, Writing - Original Draft, Writing - Review & Editing, Supervision, Resources, Funding acquisition.

Abstract

Sequential information permeates our daily lives, such as when listening to music. These sequences are potentially abstract in that they do not depend on the exact identity of the stimuli (pitch of the notes), but on the rule that they follow (interval between them). Previously, we showed that a subregion of monkey lateral prefrontal cortex (LPFC), area 46, responds to abstract visual sequences in a manner that parallels human responses. However, area 46 has several mapped subregions and abstract sequences require of multiple stimulus features (such as stimulus and time), leaving open questions as to the specificity of responses in the LPFC. To determine the anatomical and functional specificity of abstract visual sequence responses within area 46 subregions, we used awake functional magnetic resonance imaging in three male macaque monkeys during two no-report visual tasks. One task presented images in an abstract visual sequence; the other used the same timing properties and image variation, but no sequential information. We found, using subdivisions from a multimodal parcellation of area 46, that responses to abstract visual sequences were unique to the posterior fundus of area 46, which did

not respond to changes in timing or image alone. In contrast, posterior shoulder regions of area 46 showed selectivity to more concrete stimulus changes (i.e., timing and image). These results align with organizational hierarchies observed in monkeys and humans, and suggest that interactions between adjacent LPFC subregions is key scaffolding for complex daily behaviors.

Introduction

Anyone who's familiar with Beethoven's Fifth Symphony, even if you don't know it by name, will recognize the dun-dun-dun-duuuun (short, short, short, long) of the opening notes. This recognition illustrates an essential process: monitoring and tracking abstract sequences. These sequences are abstract because they do not depend on the individual stimuli. Changing the identity of the notes (e.g., by changing the key) would not affect your ability to recognize the sequence. This ability to actively track or monitor such sequences permeates our daily lives during tasks such as cooking, watching for the correct stop to exit the bus or train, and completing arithmetic problems.

While abstract sequences like music or cooking are complex and multifaceted, they can be broken down into some basic components. At minimum, they contain the abstract rule that governs the overall sequence, a timing structure, and the identity of the stimuli that compose them. Previously, we found using functional magnetic resonance imaging (fMRI) in awake macaque monkeys that abstract visual sequences were represented in a specific region of the lateral prefrontal cortex (LPFC), area 46 (Yusif Rodriguez et al. 2023). However, in this study the responses examined encompassed many potential features of the abstract sequence: rule, timing, and stimulus identity. Therefore, open questions remain as to whether specific aspects of the abstract sequence drive responses in area 46, and if and how they might be anatomically organized.

Functional specificity with respect to rule, timing, and stimulus identity is important to establish in area 46 because responses to these sequential features alone have been observed in LPFC in the past. Such features could form building blocks for conglomerate representations or be represented separately. The two features we aim to distinguish from abstract sequential rules are time and stimulus identity. For example, while the sequence rule (short, short, short, long for Beethoven's Fifth Symphony) forms the main identifying feature for abstract sequences, the identity of the items in the sequence along with their timing also constitute sequence recognition. Though different durations or pitches may not affect your general recognition of Beethoven's Fifth (as long as the same abstract 'rule' is followed), you still may notice these changes as differences from how it is classically played. Similarly, though previous responses in LPFC to abstract visual sequences were shown to be robust to changes in timing and image identity, such sequence modifications may contribute a component to the composite sequence-related response in LPFC.

Previous studies have illustrated examples of signals related to time and image identity in the LPFC that should be distinguished from those related to sequence rule. Though studies of time in monkey LPFC are not common, several studies show that electrophysiological or regional cerebral blood flow (measured with positron emission tomography, PET) responses in LPFC are modulated by the duration preceding the auditory or visual stimulus (Onoe et al. 2001; Genovesio et al. 2006; Chiba et al. 2021). LPFC has also shown responses to unpredicted changes in image identity, often referred to as "oddball" or "surprise" responses. Oddball paradigms often use simple stimulus frequency to elicit responses. Even though comparisons in our previous experiments controlled for the frequency of stimuli when examining higher-level

abstract sequential properties, it will be important to determine if responses to relatively less frequent stimuli were a component of the response in LPFC. Several studies have reported increased responses in monkey LPFC to infrequent stimuli using electrocorticography (ECoG), event-related potentials (ERPs), and awake fMRI (Chao et al. 2018; Camalier et al. 2019; Grohn et al. 2020). Thus, neural signals related to time and image identity have been observed in LPFC and it is important to determine if and how they contribute to abstract sequence representation.

Closely related to the question of functional specificity and whether features are represented in aggregate or separately is that of anatomical specificity. Monkey area 46 is relatively large, stretching the majority of the length of the principal sulcus (approx. 15 mm) along with its dorsal and ventral banks. Though seminal studies have identified subdivisions within this region (Petrides and Pandya 1984; Petrides 2005), the exact borders and subdivisions of monkey area 46, along with its relation to human area 46, have been debated and revised for decades (e.g.,Walker 1940; Petrides and Pandya 1984, 1999, 2002; Petrides 2005; Petrides et al. 2012; Rapan et al. 2023) Functional evidence has also indicated that there are subdivisions within area 46 (Tanji and Hoshi 2008; Sallet et al. 2013; Saleem et al. 2014; Ahuja and Yusif Rodriguez 2022; Jung et al. 2022; Xu et al. 2022; Rapan et al. 2023). Together, these anatomical and functional mappings indicate that there are meaningful subdivisions within monkey area 46 and thus, raise the question of how particular functional responses, such as abstract visual sequence representation, may correspond to these mappings.

Shedding light on the functional and anatomical specificity of monkey area 46 may aid in understanding the correspondence with human LPFC. According to functional connectivity

(Sallet et al. 2013), macaque area 46 is the most similar to human rostrolateral prefrontal cortex (RLPFC). RLPFC has been shown to be necessary for humans to complete abstract sequential tasks, and RLPFC shows specific dynamics in blood oxygen level dependent (BOLD) responses that increase ("ramp") through individual sequences (Desrochers et al. 2015, 2019; McKim and Desrochers 2022). These findings in humans correspond with those we previously observed in monkeys. Sequence responses in monkey area 46 showed both onset and ramping dynamics (Yusif Rodriguez et al. 2023). These studies, therefore, established sequence related ramping as an important dynamic that connects the function of monkey area 46 to human RLPFC.

Ramping is then another tool with which to examine the functional and anatomical specificity of sequence related signals in the monkey LPFC in a manner that relates to human LPFC. Ramping may also show functional distinctions with respect to sequence properties. For example, responses to time differences have been observed in neural ramping dynamics in LPFC (Niki and Watanabe 1979) and it has been shown that ramping in LPFC can be an efficient code for working memory and temporal discrimination (Cueva et al. 2020). These observations could be similar to ramping and onsets responses we previously observed in BOLD in area 46 during abstract visual sequences (Yusif Rodriguez et al. 2023). Thus, the existence of time-related responses in LPFC underscores the importance of dissociating signals related to sequences from those related to timing.

To investigate the anatomical and functional specificity of abstract visual sequence responses in monkey LPFC, we took a two-fold approach. First, we took advantage of a recent parcellation of monkey LPFC that accounted for both anatomical and functional differences across the region

(Rapan et al. 2023). We used this parcellation as the basis for mapping regions of interest (ROIs) that tiled area 46 within the LPFC. Second, to examine functional specificity, we developed a variant of the abstract sequence viewing task (hereafter abbreviated SEQ) that kept the time structure of the sequences but eliminated the ordering of visual stimuli: the Time Only (TO) task. With the TO task, we examined responses to changes in timing and images separately, i.e. not within the framework of abstract visual sequences. Given that our previous experiment made comparisons that held these variables constant, we hypothesized that the subregion of area 46 previously observed to respond to abstract visual sequence changes would be anatomically specific and would not be modulated by isolated timing or image changes in onset or ramping dynamics. Additionally, based on the responses reported by previous studies, we hypothesized that other area 46 subregions would show greater responses to changes in time, images, or both with both dynamics.

Our results broadly supported our hypotheses. Responses in the posterior fundus of area 46 (p46f) were specific to changes in abstract visual sequences and did not respond to changes in timing or image alone in both onset and ramping dynamics (as previously observed with a connectivity-based ROI (Yusif Rodriguez et al. 2023). In contrast, adjacent regions such as posterior ventral area 46 (p46v) responded to both timing and image changes with onset dynamics and posterior dorsal area 46 (p46d) responded to timing changes with ramping dynamics. These results highlight the remarkable specificity of subregions within area 46, with adjacent subregions responding to abstract and concrete changes in visual stimuli.

Methods

Participants

We tested three adult male rhesus macaques (ages spanning 6-12 years during data collection, 9-14 kg). All procedures followed the NIH Guide for Care and Use of Laboratory Animals and were approved by the Institutional Animal Care and Use Committee (IACUC) at Brown University.

Task Design and Procedure

All visual stimuli used in this study were displayed using an OpenGL-based software system developed by Dr. David Sheinberg at Brown University. The experimental task was controlled by a QNX real-time operating system using a state machine. Eye position was monitored using video eye tracking (Eyelink 1000, SR Research). Stimuli were displayed at the scanner on a 24-inch BOLDscreen flat-panel display (Cambridge Systems).

Each image presentation consisted of fractal stimulus (approximately 8° visual angle) with varying colors and features. Fractals were generated using MATLAB for each scanning session using custom scripts based on stimuli from (Kim and Hikosaka 2013) following the instructions outlined in (Miyashita et al. 1991). For each scan session, new, luminance matched fractal sets were generated. All stimuli were presented on a gray background, with a fixation spot that was always present on the screen superimposed on the images. To provide behavioral feedback, the fixation spot was yellow when the monkey was successfully maintaining fixation and red if the

monkey was not fixating. Stimuli were displayed for 0.1, 0.2, or 0.3 s each, depending on the task, sequence type, and timing template.

The timing of liquid rewards was the same across tasks and not contingent on image presentations, only on the monkey maintaining fixation. Rewards were delivered on a graduated schedule such that the longer the monkey maintained fixation, the more frequent rewards were administered (Leite et al. 2002). The first reward was given after 4 s of continuous fixation. After two consecutive rewards of the same fixation duration, the fixation duration required to obtain reward was decreased by 0.5 s. The minimum duration between rewards that the monkey could obtain was 0.5 s. Fixation had to be maintained within a small window (typically 3° of visual angle) around the fixation spot to not break fixation. The only exception was a brief time window (0.32 s) provided for blinks. If the monkey's eyes left the fixation window and returned within that time window, it would not trigger a fixation break. If fixation was broken, the reward schedule would restart at the maximum 4 s duration required to obtain reward.

Tasks were organized into runs. Runs typically lasted approximately 10 min and only one task was shown for each run. The order of tasks was pseudo-randomized within a scanning session (one day) to balance the overall number of runs for each task and their presentation order. Monkeys completed approximately 10 runs in a session.

Runs were initiated according to the monkey's fixation behavior to ensure that the monkey was not moving and engaged in the task before acquiring functional images. During this pre-scan period, a fixation spot was presented. Once the monkey successfully acquired this fixation spot

and received approximately four liquid rewards (12 – 16 s), functional image acquisition and the first habituation block were initiated. Monkeys maintained fixation for the duration of the run.

Abstract Sequence Viewing (SEQ) Task

The details of the abstract sequence viewing task have been previously described (Yusif Rodriguez et al. 2023) and are briefly summarized here. There were a total of five sequence types and nine timing templates (**Figure 1**). The inter-sequence interval was jittered to decorrelate across timing templates (mean 2 s, 0.25-8 s).

Habituation Sequences

Habituation sequences used images drawn from a pool of four fractals [A, B, C, D] and were arranged to follow one of two possible rules: three the same, one different, and four the same. All four-image sequences used one of six possible timing templates (**Figure 1C**).

Deviant Sequences

Deviant sequences used images drawn from a different pool of three fractals [E, F, G]. All deviant images were displayed for 0.2 s and used the same general timing template (adjusted for the number of items in the sequence). There were four deviant types, as follows:

- *New Items, Same Rule (NISR)*: four-image sequences that follow the same rule as the habituation sequences.
- *Rule Deviants*: four-image sequences that follow the alternate rule not used in the habituation sequences.
- *Number Deviants*: two- or six-image sequences that follow the same rule as the habituation sequences.

- *Double Deviants*: combine the rule and number deviant types and contain two- or six-image sequences that follow the alternate rule not used in the habituation sequences.

Block Structure

All blocks contained 30 sequences and an equal number of the six possible timing templates for habituation sequences. Sequences could not start with the same image as the final fractal of the previous sequence. In deviant blocks, six of the 30 sequences were deviant sequences. Deviant sequences did not occur in the first six sequences (to avoid block initiation) or consecutively. Blocks with two- and six-image sequences contained an equal number of both.

Run Structure

Each run contained five sequence blocks interleaved with 14 s fixation blocks (**Figure 1D**). The first sequence block was always all habituation sequences. The four subsequent sequence blocks each contained one type of deviant sequence. The sequential rule used for each run was counterbalanced across runs and sessions to have an equal number of each. Monkeys typically completed 4-8 runs of this task (among other tasks) in a session.

Time Only (TO) Task

The main difference between TO and SEQ was that though images were arranged into four-image groups, they were not arranged according to a sequential rule (as in SEQ) and instead displayed in pseudorandom order such that there were no repeated images. All the remaining basic structure of TO was the same as SEQ. There were the same 9 timing templates (6 habituation and 3 deviant) and two pools of fractal images (4 habituation, 3 deviant). Because there were no sequences in TO, we next detail the block types.

Block Types and Structure

All image blocks contained 30 groups of images (120 images total). The first six groups of images of a block did not contain deviant timing templates or deviant images. Each block contained key differences with respect to the composition of the timing templates and images used. There were four possible block types (**Figure 1E**), as follows:

- *Habituation Timing*: Each four-image grouping used one of the 6 possible habituation timing templates (5 of each). Images were drawn only from the habituation pool.
- *Rule Deviant Timing*: Six image groups had four-item deviant timing and the remaining 24 groups had habituation timing. The same relative fraction of images as in the SEQ task were from the deviant image pool (20%, 24 individual images), but they were randomly intermixed with images from the habituation pool.
- *Number Deviant Timing*: Six image groups had two- or six-item deviant timing (three of each) and the remaining 24 groups had habituation timing. As in Rule Timing, 20% of images were drawn from the deviant image pool and the remainder from the habituation image pool. All images were displayed in random order.
- *Novel*: As in the Habituation Timing block, each four-image grouping used one of the 6 possible habituation timing templates (5 of each). However, the images came from a novel pool of four images that had not been used in either the habituation or deviant image pools.

Run Structure

Each run was composed of four image blocks, interleaved with 14 s fixation blocks. The first block of each run was always a Habituation Timing block. The two subsequent blocks were either a Rule Timing block or a Number Timing block, with their order counterbalanced across

runs. The last block was always a Novel block. The same habituation rule was used for the entirety of a single run. Runs lasted approximately 10 min. Monkeys typically completed 2-4 runs of this task (among other tasks) in a single scanning session.

Data Acquisition

FMRI Data Acquisition

Methods are as described in (Yusif Rodriguez et al., 2022) and briefly summarized here. Monkeys sat in the "sphinx" position in an MR-safe primate chair (Applied Prototype, Franklin, MA or custom-made by Brown University) with their head restrained using a plastic "post" (PEEK, Applied Prototype, Franklin, MA) affixed to the monkeys' head and the primate chair. Monkeys wore earplugs during MRI scanning (Mack's Soft Moldable Silicone Putty Ear Plugs, "kid's" size). Monkeys were habituated to all scanning procedures prior to the MRI scanning sessions.

Approximately 30-60 min prior to each scanning session, monkeys were intravenously injected with a contrast agent: monocrystalline iron oxide nanoparticle (MION, Feraheme (ferumoxytol), AMAG Pharmaceuticals, Inc., Waltham, MA, 30 mg per mL or BioPal Molday ION, Biophysics Assay Lab Inc., Worcester, MA, 30 mg per mL). MION was injected into the saphenous vein below the knee (7 mg/kg), then flushed with a volume of sterile saline approximately double the volume of the MION injected. No additional MION was added during scanning.

A Siemens 3T PRISMA MRI system with a custom six-channel surface coil (ScanMed, Omaha, NE) at the Brown University MRI Research Facility was used for whole-brain imaging.

Anatomical scans consisted of a T1-MPRAGE (repetition time, TR, 2700 ms; echo time, TE, 3.16 ms; flip angle, 9°; 208 sagittal slices; 0.5 x 0.5 x 0.5 mm), a T2 anatomical (TR, 3200 ms; TE 410 ms; variable flip angle; 192 interleaved transversal slices; 0.4 x 0.4 x 0.4 mm), and an additional high resolution T2 anatomical (TR, 8020 ms; TE 44 ms; flip angle, 122°; 30 interleaved transversal slices; 0.4 x 0.4 x 1.2 mm). Functional images were acquired using a fat-saturated gradient-echoplanar sequence (TR, 1.8 s; TE, 15 ms; flip angle, 80°; 40 interleaved axial slices; 1.1 x 1.1 x 1.1 mm).

Data Analysis

All preprocessing and data inclusion criteria are the same as in (Yusif Rodriguez et al. 2023). Most analyses were performed in Matlab using SPM 12 (http://www.fil. Ion.ucl.ac.uk/spm). Prior to analysis, data were preprocessed using the following steps: reorienting (to ensure proper assignment of the x,y,z planes), motion correction (realignment), normalization, and spatial smoothing (2 mm isotropic Gaussian kernel separately for gray matter and white matter). All steps were performed on individual runs separately. The T1-MPRAGE anatomical image was skull stripped using FSL BET brain extraction tool (http://www.fmrib.ox.ac.uk/fsl/) to facilitate normalization. All images were normalized to the 112-RM SL macaque atlas (McLaren et al., 2009).

Runs were included for analysis only if they met the following criteria: the monkey had to be performing well and a sufficient number of acquisition volumes within the run had to pass data quality checks. The monkey's performance was evaluated by calculating the percentage of time within a run that fixation was maintained. Runs were excluded if the monkey was fixating < 80%

of the time. We used the ART toolbox (Artifact Detection Tools, https://www.nitrc.org/projects/artifact_detect) to detect outlier volumes (standard global mean; global signal detection outlier detection threshold = 4.5; motion threshold = 1.1mm; scan to scan motion and global signal change for outlier detection). Any run with greater than 12% of volumes excluded was excluded from analysis (**Table 1**).

FMRI Models

For all models, data were binned to evenly distribute included runs from the SEQ and TO tasks (**Table 1**) into pseudo-subject bins. Each bin contained data from only one monkey and distributed runs from the SEQ and TO tasks as evenly as possible. Each bin contained approximately 20 SEQ and 10 TO runs. Runs from earlier and later scanning sessions were pseudorandomly distributed across bins. For the SEQ task, both rule types (AAAA and AAAB) were evenly distributed in each bin. This binning procedure resulted in 11 total pseudo-subject bins.

Within-subject statistical models were constructed under the assumptions of the general linear model (GLM) in SPM 12 for each pseudo-subject bin. Condition regressors were all convolved with a gamma function (shape parameter = 1.55, scale parameter = 0.022727) to model the MION hemodynamic response function (Vanduffel & Farivar, 2014). The first six image groups (24 images) and reward times were included as nuisance conditions. Additional nuisance regressors were included for the six motion estimate parameters (translation and rotation) and image variability (standard deviation of within-run image movement variability, calculated using the ART toolbox). Outlier volumes determined with the ART toolbox in preprocessing were

"scrubbed" by adding an additional regressors, each with a "1" only at the volume to be excluded.

Regressors were estimated using a bin-specific fixed-effects model. Whole-brain estimates of bin-specific effects were entered into second-level analyses that treated bin as a random effect. One-sample t-tests (contrast value vs zero, $p < 0.005$) were used to assess significance. These effects were corrected for multiple comparisons when examining whole-brain group voxelwise effects using extent thresholds at the cluster level to yield false discovery rate (FDR) error correction ($p < 0.05$).

The following two GLMs were used for analyses:

Onsets Model

To assess the univariate effects of deviant sequences, we constructed a model using instantaneous stimulus onset regressors. Both tasks were modeled simultaneously, with runs from both tasks included in each pseudo-subject bin. For the SEQ task, onsets were modeled similarly as described in Yusif Rodriguez, et al. (2023). Onsets were modeled at the first item in each sequence type. Habituation and deviant sequences were modeled separately. Habituation sequences were divided by timing template (short, medium, and long) and whether they came from the first block containing only habituation sequences or a subsequent block that contained deviant and habituation images, yielding six total habituation sequence regressors. Deviant sequences were modeled separately according to their type: NISR, rule deviants, number deviants (two- and six-image), and double deviants (two- and six-image), yielding six total deviant sequence regressors. In total, the SEQ task contained 12 condition regressors (**Table 2**).

For the TO task, onsets were modeled for the first item in each group of images (a single timing template). Habituation and deviant timing templates were modeled separately. As in the SEQ task, habituation timing templates were divided by those occurring in the first block (where there were no deviant timing templates or images) and those occurring in subsequent blocks that contained deviant images and timing templates. Habituation timing templates were again divided by short, medium, and long yielding a total of six habituation timing template regressors. Deviant timing templates were modeled separately as rule timing (four images) and number timing (two- and six-images), yielding three total deviant timing template regressors. Deviant images that were randomly interspersed in blocks that contained timing template deviants were modeled separately at the onset of each individual deviant image. The novel image block was also separately modeled and divided by the three habituation timing templates (short, medium, long); however, these were not included in analyses. In summary, the TO task contained six habituation time, three deviant time, one deviant image, and three novel image regressors for a total of 13 regressors (**Table 2**).

Ramp Model

Previously, we showed that variance attributable to a ramping dynamic is separable from that attributed to a change at the last item in the sequence by using two parametric regressors (modeled stepwise) with the unique variance assigned to ramping (Yusif Rodriguez et al. 2023). We used this same parametric last item versus unique ramp model here and will refer to it as the ramping model.

Across both tasks, for each group of images the first regressor was an instantaneous onset at each image, the last item parametric was added as ones for the first images and an arbitrarily larger value (6) at the last image, and the ramp parametric that monotonically increased for each image (e.g., 1, 2, 3, 4). These were modeled stepwise such that the final ramp parametric would be assigned the unique variance that is above and beyond what can be explained by onsets or a change at the last item. Nuisance regressors did not include parametrics.

In each task, the conditions were the same as described for the Onsets Model. For the SEQ task this included six habituation sequence conditions and six deviant sequence conditions. In the TO task there were six habituation time conditions, three deviant time conditions, deviant images, and three novel image conditions that were modeled with parametrics.

ROI Analysis

Individual area 46 subregion ROI images were directly acquired from the MEBRAINS Multilevel Macaque Atlas https://search.kg.ebrains.eu/instances/Project/e39a0407-a98a-480e-9c63-4a2225ddfbe4. Individual subregion image warps were created from their native space to 112RM-SL space using Rhemap (Sirmpilatze and Klink 2020, https://github.com/PRIME-RE/RheMAP). Individual warps were then applied to create images used in ROI analysis for the following subregions: a46v, a46d, p46v and p46d (**Figure 2**). Because the ROI used in (Yusif Rodriguez et al. 2023) spanned subregions p46df and p46vf and responses in these subregions were not distinct, for simplicity, we combined subregions in the fundus of area 46 to create a46f (a46df + a46vf) and p46f (p46df + p46vf).

To compare activation within and across ROIs in a manner that controlled for variance, we extracted t-values from the condition of interest over baseline using the Marsbar toolbox (Jean-Baptiste Poline, 2002). T-values (one for each pseudo-subject bin: n = 11 bins) were entered into RM-ANOVAs with the identity of the monkey entered as a covariate.

Results

Three male monkeys (Macaca mulatta) performed a no-report abstract sequence viewing task (abbreviated SEQ hereafter) that contained a visual sequence rule and structured timing (previously reported on in Yusif Rodriguez, et al., 2023), and a variant of this task, termed time only (TO), while undergoing awake fMRI scanning (**Figure 1**). In both tasks, the monkeys were required to fixate a central spot while viewing streams of fractal images arranged into groups of four items or the fixation spot alone. Neither task required responses, only fixation, and therefore both were "no-report". The tasks were performed in runs (~10 min each). Runs were divided into blocks that were task-specific and interleaved with 14-s fixation blocks. In SEQ, task blocks contained 30 sequences each. In TO, task blocks contained four-item groupings where the images were presented in pseudo-random order. Reward delivery was not correlated with sequence presentation and was delivered on a graduated schedule to encourage animals to maintain fixation throughout the run. The longer animals maintained fixation, the shorter the duration between rewards. Monkeys performed the task well and fixated for 95% and 96% of the time in included runs in SEQ and TO, respectively (see Methods for those excluded).

Our main goals were to 1) test anatomical specificity in whether sequence related responses previously observed in area 46 of DLPFC were unique to a specific subregion of area 46; 2) test functional specificity in whether similar responses would be observed in the absence of a visual sequential rule; and 3) to determine if there is anatomical and functional specificity in sequence related dynamics that parallel those in humans (ramping). A growing body of literature has highlighted both anatomical and functional distinctions across DLPFC subregions (Rapan et al. 2023). Further, previous work has identified networks in the frontal cortex that are involved in processing timing structures (Onoe et al. 2001; Genovesio et al. 2006; Chiba et al. 2021), raising the possibility that the structured timing could be a component of the neural response in the DLPFC.

To accomplish these goals, deviant responses were used as an index into abstract sequence representation, as in previous studies (Wang et al. 2015; Yusif Rodriguez et al. 2023). That is, if there was a change in the abstract sequence, then that change would be reflected in a change in the activity of a region if there was a representation of the abstract sequence present. In the SEQ task, the primary two comparisons were rule deviants and number deviants compared to new items of the same rule. In both comparisons all images came from the same deviant pool and therefore controlled for a response solely driven by less frequent images. Double deviants were included to counterbalance the design but were not included for analysis. In the TO task, the medium four-item deviant timing template and the two- and six-item timings were the relevant deviants.

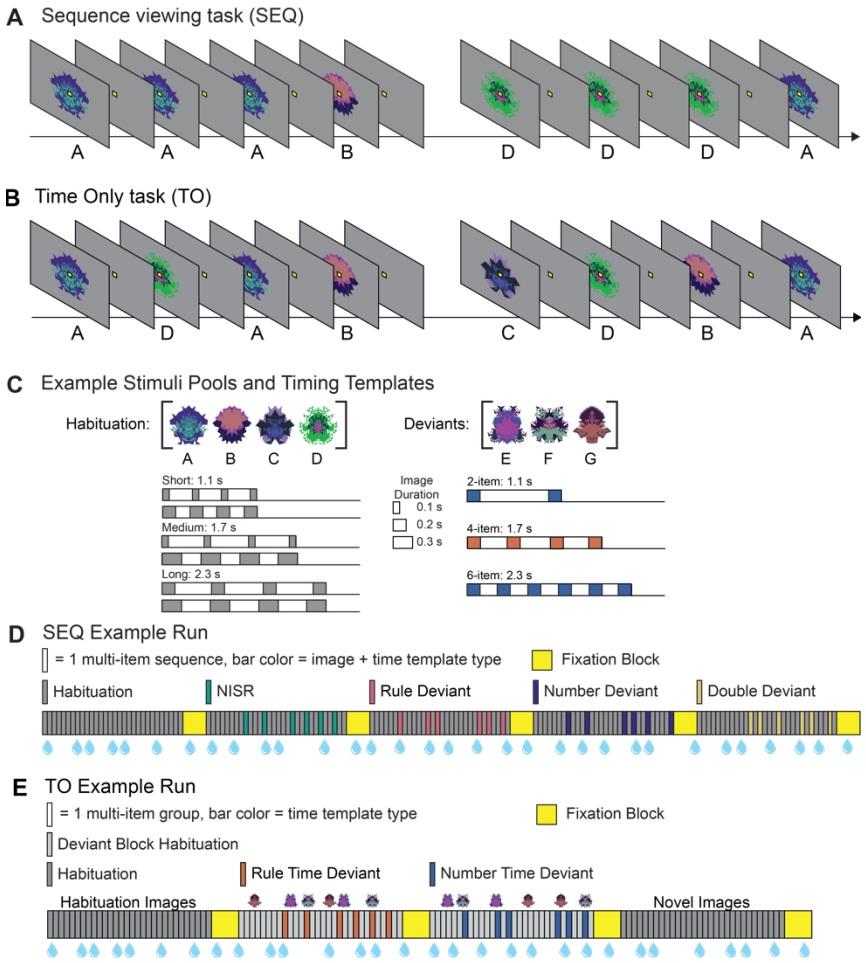

Figure 1. Sequence viewing task (SEQ) and Timing only (TO) task structure. A. Example partial habituation block from SEQ task for sequence rule *three same, one different* (AAAB) and habituation timing templates. **B.** Example partial habituation block from TO illustrating non-sequential structure and habituation timing templates. **C.** Example stimulus pools (top) show a set of images that would be used in a single scanning session for both tasks. TO additionally contains a novel images category, with different images not exemplified here. New images are used each session. Six possible habituation event timing templates (bottom, left) and deviant event timing templates (bottom, right) illustrated with gray rectangles indicating individual image presentations. Total sequence durations are listed for each template type. **D.** Example SEQ run, with each bar indicating one multi-image sequence: four images in habituation, new items same rule (NISR), and rule deviants; two or six images in number and double deviants. The first block contains only habituation sequences and subsequent blocks contain only one of the four deviant types. **E.** Example TO run, with each bar indicating a multi-image set grouped by timing template. In the TO

task, miniaturized fractal deviant markers exemplify pseudorandom individual deviant image presentations within relevant blocks. Task relevant blocks alternate with fixation blocks for both SEQ and TO tasks. Blue water droplets schematize reward delivery, which is decoupled from sequence viewing and delivered on a graduated schedule based on the duration the monkey has maintained fixation.

The fundus of monkey DLPFC area 46 represents abstract visual sequences

To address the first question, of anatomical specificity and whether sequence representations were unique to subregions of area 46 within the DLPFC, we used new regions of interest (ROI) that tiled area 46 and replicated previous analyses during the SEQ task (Yusif Rodriguez, et al., 2023). First, to tile area 46 we used the MEBRAINS Multilevel Macaque Brain Atlas (Rapan et al. 2023; Balan et al. 2024)that parcellated area 46 according to cytoarchitectonic divisions augmented by functional connectivity and neurochemical data. This atlas divides area 46 into eight distinct regions (four anterior and four posterior) that are then divided into dorsal and ventral shoulder and fundus regions (**Figure 2A**,**B**). Of the area 46 subdivisions, the posterior fundus (p46df and p46vf) regions showed the greatest overlap with the previous R46 ROI constructed from functional connectivity seed coordinates (Sallet et al. 2013; Yusif Rodriguez et al. 2023) (**Figure 2C**). Of the 895 voxels in the previous R46 ROI, 40.5% (420) overlapped with cortical gray matter, and all of those voxels overlapped with p46df and p46vf combined. We therefore combined the fundus regions and focused our analyses on the posterior fundus (p46f). We compared p46f to the other five regions: anterior dorsal (a46d), anterior fundus (a46f), anterior ventral (a46v), posterior dorsal (p46d), and posterior ventral (p46v).

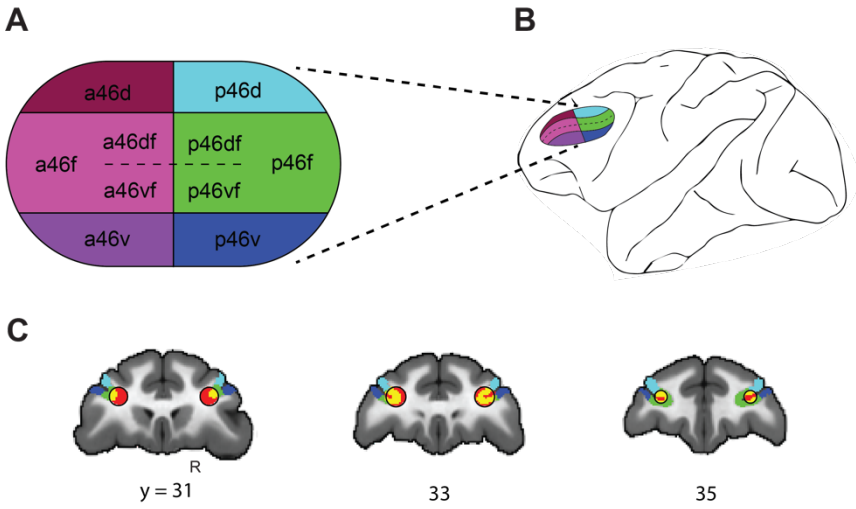

Figure 2. Schematic of anatomical subdivisions of area 46. A. Schematic of the area 46 subregions in the DLPFC examined in this study based on the atlas by Rapan et al. 2023. All subregions use the following naming convention: a-anterior, p-posterior, d-dorsal, v-ventral and f-fundus. Dashed line schematizes the fundus of the principle sulcus and notes the distinction between dorsal and ventral fundus regions that were identified in the atlas but combined for the purposes of this study. **B.** Same cortical subregions illustrated in **A** schematized on the left lateral surface of the macaque brain. **C.** Coronal slices displaying the area 46 ROI sphere used in Yusif Rodriguez et, al. 2023 (red, outlined in black) superimposed on the ROIs used for analysis in this study (light blue, blue and green, corresponding to regions illustrated in **A**). Yellow voxels indicate overlap between the previous red sphere and current p46f (green).

To replicate our previous analyses and examine neural (blood oxygen level dependent, BOLD) activity for this and subsequent questions, we created two models, one for onsets and one for ramping (see Methods for details). Each model contained both the SEQ and TO tasks, with separate regressors for each habituation and deviant timing template, modeled as zero-duration onsets. Statistical testing was performed on approximately 20-run bins (n = 11), each consisting of data from a single monkey. For each condition, t-values were extracted for that condition compared to baseline (e.g., SEQ-Rule Deviant > Baseline) to account for potential differences in variance across conditions. These values were used to examine ROI activity throughout, and we

refer to comparisons by the condition of interest (i.e., without listing the contrast over baseline, e.g., SEQ-Rule Deviant). All statistical tests on ROIs were performed on binned data and included a covariate for monkey identity (n = 3). While we report the effect of variation between monkeys in the following analyses, the main focus of the study was not on individual differences, and our discussion focuses on condition effects.

In the SEQ task, the main conditions of interest were the deviant responses. Deviant responses were used as an index into abstract sequence representation, as in previous studies (Wang et al. 2015; Yusif Rodriguez et al. 2023). That is, if there was a change in the abstract sequence, then that change would be reflected in a change in the activity of a region if there was a representation of the abstract sequence present. To test for abstract sequence representation, the primary two comparisons were rule deviants (SEQ-Rule Deviant) and number deviants (SEQ-Number Deviant) compared to new items of the same rule (NISR) in the SEQ task. In both comparisons, all the images were from the same deviant pool and therefore controlled for a response solely driven by less frequent images. Double deviants were included to counterbalance the design but were not included for analysis.

To begin to address the question of anatomical specificity of abstract visual sequence representations, we first focused on replicating results in the subregion of area 46 that showed the greatest overlap with the ROI used in the previous study, p46f (**Figure 2**). Previously we found that visual abstract sequence deviant responses were primarily on the right with onset dynamics. We verified that with slightly different onset models (that included both SEQ and TO tasks), responses to both SEQ-rule (**Figure 2A**, $p < 0.01$) and SEQ-number (**Figure 2B**, $p <$

0.04) deviants were both significantly greater than NISR in right p46f (see **Table 3** for full statistics). Also similar to previous results, deviant responses in left p46f were not significantly different from NISR (SEQ-rule > NISR: $F_{(1,8)} = 4.3$, $p = 0.07$, $\eta_p^2 = 0.35$; SEQ-number > NISR: $F_{(1,8)} = 0.52$, $p = 0.5$, $\eta_p^2 = 0.06$), but they were not reliably different from those in right p46f for TO-rule deviants (SEQ-rule > NISR Left Vs. Right: $F_{(1,18)} = 0.92$, $p = 0.35$, $\eta_p^2 = 0.05$; SEQ-number > NISR Left Vs. Right: $F_{(1,18)} = 6.27$, $p = 0.02$, $\eta_p^2 = 0.26$). As expected, these results were supported by whole brain contrasts of SEQ-Rule Deviants > NISR (**Figure 2C**) and SEQ-Number Deviants > NISR (**Figure 2D**) in the SEQ task (**Table 4**). Both deviant types showed significant clusters of activation in right p46f. We also observed a significant cluster spanning left p46v/p46vf. Therefore, we replicated deviant responses in p46f onset dynamics during the SEQ task.

Our next goal was to determine the anatomical specificity of the onset deviant responses in right p46f. Previous work has demonstrated that area 46 contains anatomical and functional subdivisions (Tanji and Hoshi 2008; Sallet et al. 2013; Saleem et al. 2014; Ahuja and Yusif Rodriguez 2022; Jung et al. 2022; Xu et al. 2022; Rapan et al. 2023). The involvement of these subregions in abstract visual sequence representation was previously unstudied, leaving the specificity of these responses an open question. Therefore, we compared the p46f subregion to the five other subregions in area 46. Only two subregions showed reliable differences for SEQ-rule deviants compared to NISR: right p46f and p46d (**Figure 3A**). These two ROIs were not different from each other in their responses (ROI x condition: p = 0.53, **Table 5**). In planned comparisons to other subregions, we found that p46f was marginally different from a46d, a46v, and p46v (p's < 0.10, orange axes highlights, **Figure 3A**) while there was no reliable difference

between p46f and a46f ($p = 0.31$). Similar trends were observed for SEQ-number deviants compared to NISR (**Table 5**). The p46f subregion was the only area showing a reliably greater response for number deviants compared to NISR (**Figure 3B**). The response in p46f was significantly different from that in a46d (which was significantly different in the opposite direction, ROI x condition: $p < 0.001$), a46f ($p < 0.05$), and p46v ($p < 0.02$), and marginally different from a46v ($p < 0.07$). These results suggest that activity in posterior area 46 may be uniquely biased to represent changes in abstract visual sequences.

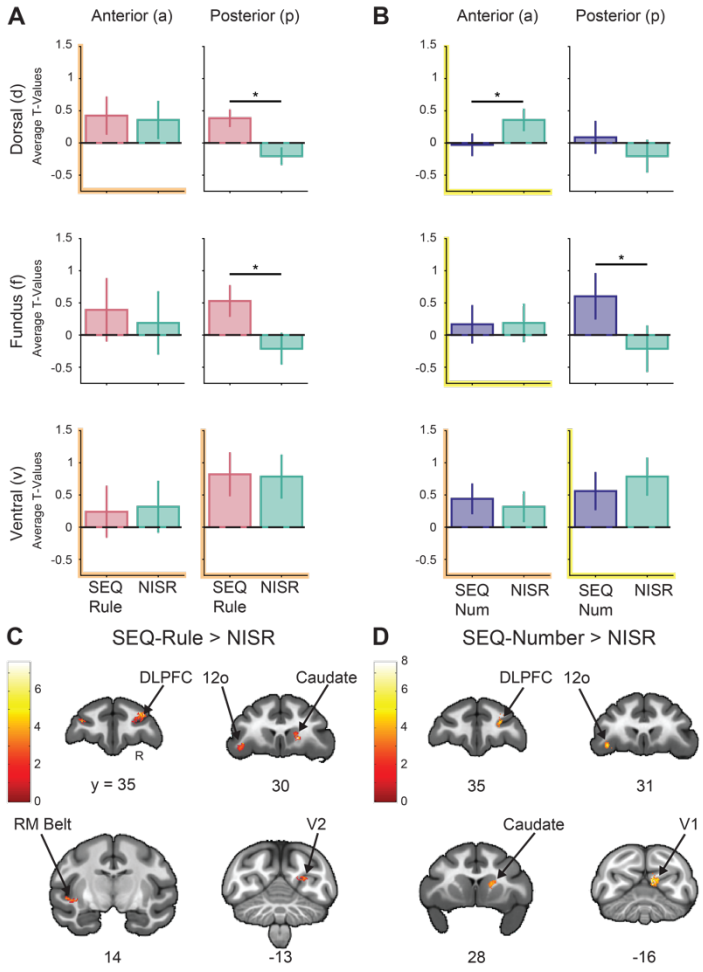

Figure 3. Posterior right area 46 fundus in SEQ task shows onset deviant responses. (A and B) T-values for the condition of interest > baseline are shown. Left column indicates anterior regions and the right indicates posterior regions. First row corresponds to dorsal, second to fundus and third to ventral regions. Error bars are 95%

confidence intervals (1.96 x standard error of the within-bin mean). Asterisks in graphs indicate significance within comparisons and highlighted axes denote significant (yellow) or marginally significant (orange) interaction of subregion and condition when compared to p46f. **A.** SEQ-Rule deviants compared to new items, same rule (NISR) across DLPFC subregions. SEQ-Rule deviants compared to NISR in p46d and p46f showed a reliable difference. The response in p46f was marginally different from those in a46d, a46v, and p46v. **B**. SEQ-Number deviants compared to NISR across DLPFC subregions. SEQ-Number deviants compared to NISR in a46d and p46f showed a reliable difference. The response in p46f was significantly different from a46d, a46f, and p46v and marginally different from a46v. **C.** Voxel wise contrast of SEQ-Rule Deviants > NISR false discovery rate (FDR) error cluster corrected for multiple comparisons (FDRc < 0.05, height p < 0.005 unc., extent = 100) are shown. **D.** Voxel wise contrast of SEQ-Number Deviants > NISR false discovery rate (FDR) error cluster corrected for multiple comparisons (FDRc < 0.05, height p < 0.005 unc., extent = 133) are shown. Color bar indicates T-values in **C** and **D**.

In parallel with our goal of determining the anatomical specificity of LPFC responses in onset dynamics, we aimed to determine the anatomical specificity of ramping dynamics. Ramping dynamics are necessary in humans during abstract sequential tasks (Desrochers et al. 2015, 2019; McKim and Desrochers 2022) and are located in the RLPFC, which functional connectivity suggests is homologous to monkey p46f (Sallet et al. 2013). Previously, we observed that ramping was reliably different for rule deviants compared to NISR, primarily in left area 46. First, to replicate those previous results, we constructed the same ramping model that isolated an increase across the items in the sequence from an increase only at the last item as previous but included both tasks (see Methods). We examined activity in the left p46f during the SEQ task and found similar trends as previously observed (**Figure 4**). Ramping during SEQ-rule and SEQ-number deviants was numerically greater than NISR, however in this ROI they did not reach statistical reliability (SEQ-rule: p = 0.23, SEQ-number: p = 0.15; **Table 6**). Regardless, results from the whole-brain analysis do replicate previous results and show a reliable cluster of

activation in left area 46 (**Figure 4C**, **Table 7**). This cluster spans several left area 46 dorsal subregions: a46d, p46d, and p46df. Therefore, we replicated the presence of ramping activation in a small, but distinct, set of subregions of left area 46, even though it was not strictly localized to p46f.

Having replicated the general presence of ramping activation in response to abstract sequence deviants in left area 46, we examined the anatomical specificity of this response. Though the difference in ramping response between SEQ-rule deviants and NISR within the p46f ROI alone was not reliable, it was the only ROI where the ramping response to SEQ-rule was positive (as in humans and previous results). Therefore, we reasoned that it would still be informative to compare p46f to the other five subregions. In planned comparisons we found that ramping to SEQ-rule deviant responses in p46f were reliably different from those in all anterior subregions: a46d, a46f, and a46v (ROI x condition: p's < 0.04, **Figure 4A**, **Table 8**). Responses in p46f were not reliably different from other posterior subregions: p46d and p46v (p's > 0.18). In contrast to SEQ-rule ramping responses, comparisons between p46f and other subregions for SEQ-number deviant vs. NISR ramping responses did not yield any reliable differences (p's > 0.22, **Table 8**). This result was expected given the lack of general ramping responses in left area 46 to SEQ-number deviants. Together, these results suggest that ramping SEQ-rule deviant responses are unique to left posterior area 46.

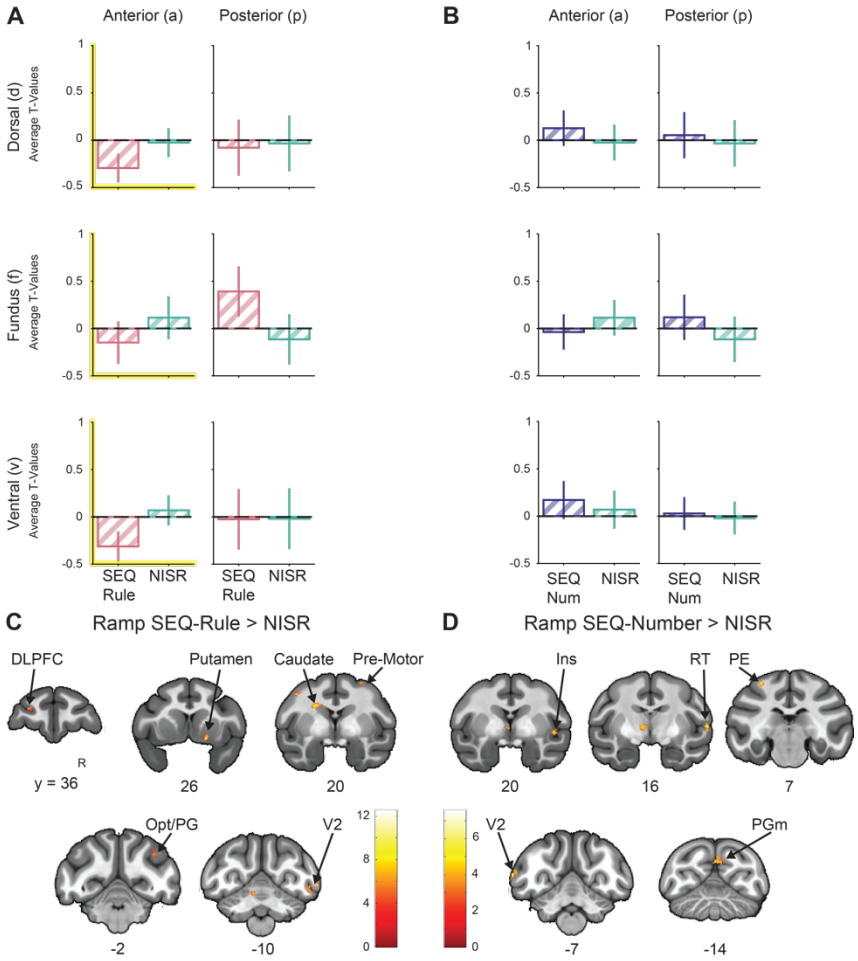

Figure 4. Posterior right area 46 fundus in SEQ task shows ramping activity during deviants. (**A and B**) T-values for the condition of interest > baseline are shown. Left column indicates anterior regions and right indicates posterior regions. First row corresponds to dorsal, second to fundus and third to ventral regions. Error bars are 95% confidence intervals (1.96 x standard error of the within-bin mean). Asterisks in graphs indicate significance within comparisons and highlighted axes denote significant (orange) or marginally significant (yellow) interaction of subregion and condition when compared to p46f. **A.** Ramping activity for SEQ-rule deviants compared to new items, same rule (NISR) across DLPFC subregions. Responses in p46f were significantly different from those in a46d, f, and v. **B**. Ramping activity for SEQ-number deviants compared NISR across described DLPFC subregions. **C.** Voxel wise contrast of ramping activity in SEQ-Rule Deviants > NISR false discovery rate (FDR) error cluster corrected for multiple comparisons (FDRc < 0.05, height $p < 0.005$ unc., extent = 84) are shown. **D.** Voxel wise contrast of ramping activity in SEQ-Number Deviants > NISR false discovery rate (FDR) error cluster corrected for

multiple comparisons (FDRc < 0.05, height p < 0.005 unc., extent = 74) are shown. Color bar indicates T-values in **C** and **D**.

Time deviants do not elicit activity in the posterior fundus of area 46

We next tested the functional specificity of the deviant response itself in area p46f. Previous studies showed that regions of the frontal cortex process different types of timing structures (Onoe et al. 2001; Genovesio et al. 2006; Chiba et al. 2021), raising the possibility that a difference in the timing structure alone could be a component of the deviant response. All SEQ task deviants used a timing template (0.2 s image duration for medium, 1.7 s, total duration) that was different from the timing templates used for habituation sequences in SEQ. To determine if deviants in timing structure alone could drive p46f responses, we compared responses to deviant timing templates to habituation timing templates in the TO task. The same timing templates were used in the TO task as in the SEQ task; however, the serially displayed fractal images did not follow a sequential abstract rule and instead were pseudo-randomly assigned such that there were no image repeats (**Figure 1**). The first block in the TO task contained only habituation images (in random order) and habituation timing templates as in the SEQ task. Subsequent deviant blocks in the TO task contained six deviant timing templates and 20% of images were from the deviant image pool (randomly interleaved with habituation pool images), mirroring the structure of the SEQ task. All comparisons between habituation timings and deviant timings came from deviant blocks and therefore contained the same fraction of deviant images. Thus, the structure of the TO task was as closely matched to the SEQ task as possible such that the only difference was the ordering of the images.

To determine if deviant timing structures could elicit onset responses in right area p46f where we observed SEQ-deviant onset responses, we compared responses to deviant timing structures to habituation timing structures in the TO task. We will refer to four-item timing template deviants as TO-rule deviants; two- and six-item timing template deviants as TO-number deviants; and the habituation timing templates from deviant blocks that they will be compared to as TO-habituation. We found that changes in timing structure alone did not elicit deviant responses in right p46f. There were no reliable differences between TO-rule deviants ($p = 0.86$, **Figure 5A**) or TO-number deviants compared to TO-habituation ($p = 0.85$, **Figure 5B**, see **Table 9** for full stats). These results were supported by whole brain contrasts showing no significant clusters of activation in p46f when contrasting TO-rule and TO-number deviants to TO-habituation (**Figure 5C,D**, **Table 10**). Together, these results suggest that a deviation in timing template only, without the presence of an abstract visual sequence, does not elicit responses in p46f.

However, there were other regions within right area 46 that showed significant responses to changes in timing template. For TO-Rule compared to TO-habituation, a46d, a46f, and p46v all showed reliable differences (p's < 0.03, **Figure 5A**, **Table 9**). Notably, p46v also showed reliable differences between TO-Number and TO-habituation ($p < 0.01$, **Figure 5B**), and for all the reliable differences the onset responses TO-habituation were greater than to those of the TO-rule and -number deviants. These results were underscored by comparisons between p46f and the other five subregions. Overall responses were greater in p46v than p46f (main effect of ROI $p < 0.01$, **Table 11**) and the difference between TO-deviant and TO-habituation was significantly different by ROI for TO-number and marginal for TO-rule (ROI x condition: $p < 0.09$, **Table 11**). These results were supported by those in whole brain contrasts (**Figure 5C,D**). Additionally,

several regions including the frontal cortex, showed greater responses to TO-rule and -number deviants than TO-habituation. TO-Rule Deviant > TO-Habituation showed significant clusters in regions such as the temporal pole, TPO, putamen, cerebellum, and visual cortex (V1, V2). TO-Number Deviant > TO-Habituation showed significant regions of activation in frontal cortex (dorsal area 9, area 13m and F5 of premotor) along with area MT, area TEpv, and visual areas (V1, V2). Thus, timing responses in p46v functionally dissociated from sequence specific responses in the adjacent p46f and may be part of a larger network of areas that is specialized to detect timing differences, independent of abstract sequential structure.

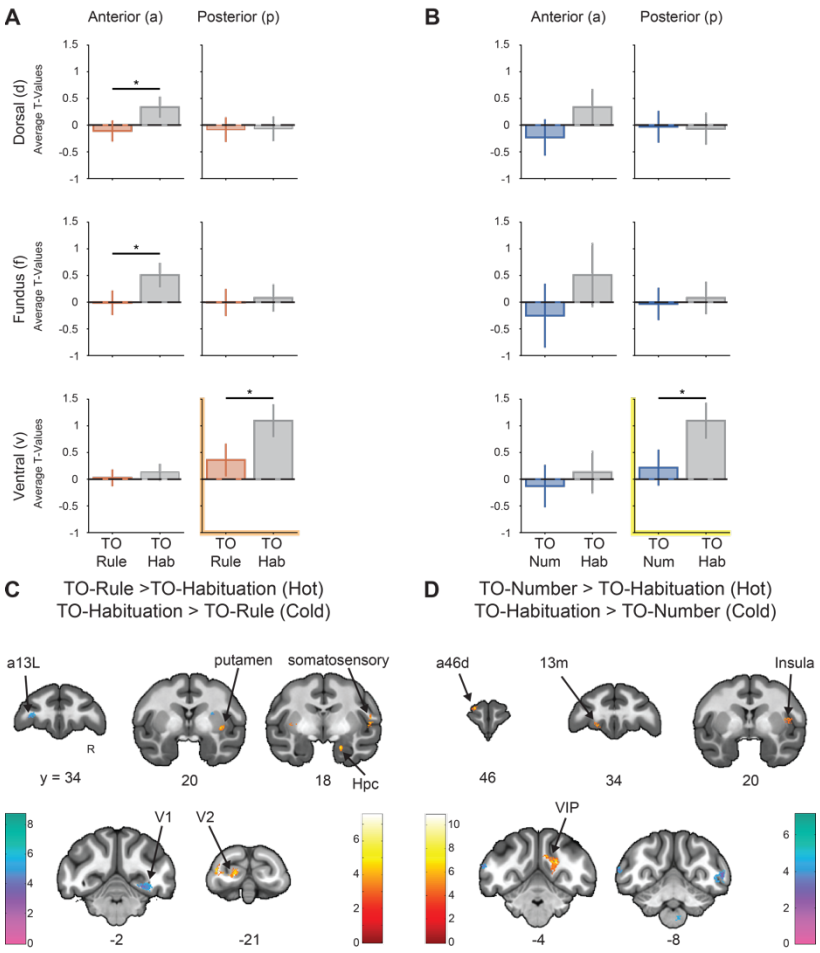

Figure 5. **Right p46v and not p46f showed onset responses to TO-rule and -number deviants. (A and B)** T-values for the condition of interest > baseline are shown. Left column indicates anterior regions and right indicates posterior regions. First row corresponds to dorsal, second to fundus and third to ventral regions. Error bars are 95% confidence intervals (1.96 x standard error of the within-bin mean). Asterisks in graphs indicate significance within comparisons and highlighted axes denote significant interaction of subregion and condition when compared to p46f. **A.** TO-rule deviants compared to TO-habituation across subregions showed reliable differences in a46d, a46f and p46v. Additionally, responses in p46f were marginally different from p46v. **B**. TO-number deviants compared to TO-habituation across subregions showed a reliable difference in p46v that was significantly different from the response in p46f. **C.** Voxel wise contrasts of TO-Rule Deviant > TO-Habituation (Hot colors) false discovery rate (FDR) error cluster corrected for multiple comparisons (FDRc < 0.05, height $p < 0.005$ unc., extent = 84), overlayed with TO-Habituation > TO-Rule Deviant (Cold colors) false discovery rate (FDR) error cluster corrected for

multiple comparisons (FDRc < 0.05, height p < 0.005 unc., extent = 204) are shown. **D.** Voxel wise contrasts of TO-Number Deviant > TO-Habituation (Hot) false discovery rate (FDR) error cluster corrected for multiple comparisons (FDRc < 0.05, height p < 0.005 unc., extent = 94), overlayed with TO-Habituation > TO-Number Deviant (Cold) false discovery rate (FDR) error cluster corrected for multiple comparisons (FDRc < 0.05, height p < 0.005 unc., extent = 104) are shown. Color bars indicate T-values in **C** and **D**.

Now that we had determined that onset responses were functionally specific within right area 46 subregions, we again turned to our parallel question of whether ramping dynamics would also be functionally specific to left area 46. This question was further motivated by observations from previous studies that ramping responses have specifically been associated with timing in the frontal cortex of monkeys (Onoe et al. 2001; Genovesio et al. 2006; Chiba et al. 2021) and by the fact that ramping and onset dynamics can reflect different task information in humans (Desrochers et al. 2015, 2019; McKim and Desrochers 2022). To answer this question, we performed the same analysis of TO-rule and -number deviants with ramping activation in left area 46 as we did with onsets in right area 46. Here, we also found that ramping responses to timing deviants alone were not present in p46f. There were no reliable differences between TO-rule or TO-number deviants and TO-habituation (p's > 0.25, **Figure 6A,B**, see **Table 12** for full stats). These results were supported by whole-brain contrasts. Contrasts of TO-Rule Deviants > TO-Habituation and TO-Number Deviants > TO-Habituation both showed no significant clusters in p46f (**Figure 6C,D**, **Table 13**). These results suggest that deviant ramping responses in left p46f are specific to changes in abstract visual sequence rule.

However, as in the onsets, there were differences in ramping in areas outside of p46f for time deviants, illustrating our ability to detect such changes and the functional specificity within left

area 46 for ramping dynamics. The only area 46 subregion that showed reliably different ramping responses to TO-rule and TO-number deviants compared to TO-habituation was p46d for both comparisons. However, ramping responses to different timing templates for left p46f were not reliably different from p46d or the other area 46 subregions (p's > 0.21, **Table 14**). This observation was not to the exclusion of areas in the rest of the brain, which did show significant clusters of activation for changes in ramping related to timing. These regions included: caudate, pre-motor cortex, insula, anterior lateral belt, area V4, cerebellum, motor cortex, and temporal area TA (**Figure 6C,D**, **Table 13**). Many of these regions were similar to those observed in onset dynamics. In summary, changes in timing structure alone were not sufficient to elicit deviant ramping responses in left p46f, indicating that responses there are functionally distinct from nearby regions such as p46d and potentially associated networks in the brain at large that did show changes in ramping dynamics in response to changes in timing.

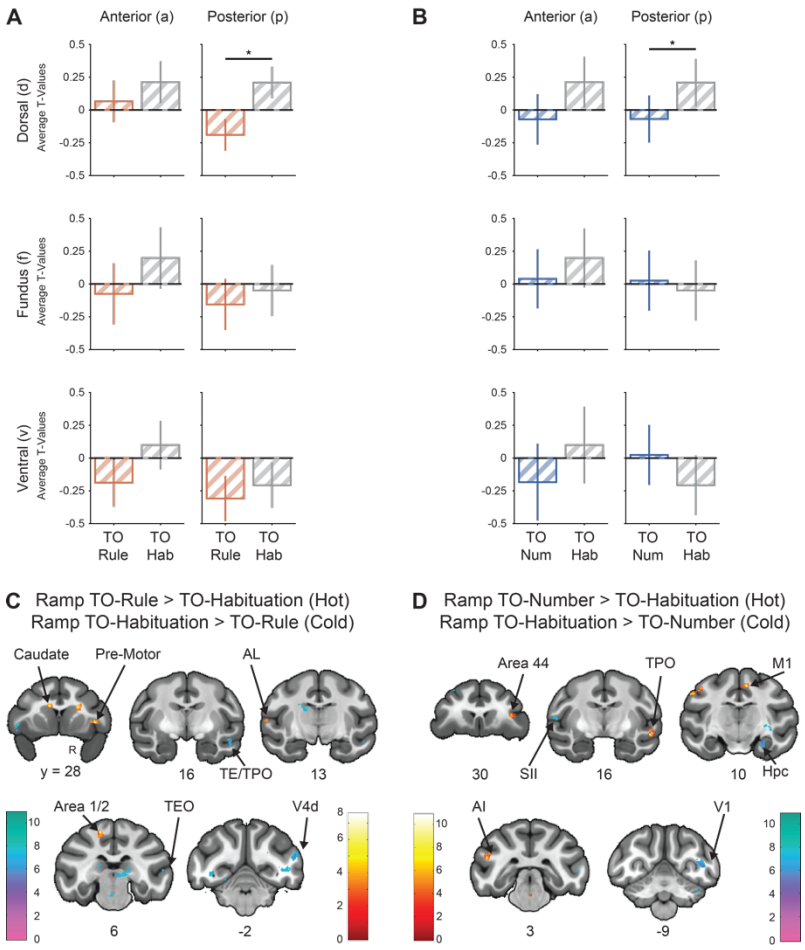

Figure 6. Left p46d and not p46f shows ramping responses to timing template deviants in the TO task. (**A and B**) T-values for the condition of interest > baseline are shown. Left column indicates anterior regions and the right indicates posterior regions. First row corresponds to dorsal, second to fundus and third to ventral regions. Error bars are 95% confidence intervals (1.96 x standard error of the within-bin mean). Asterisks in graphs indicate significance within comparisons. **A**. Ramping activation in TO-rule deviants compared to TO-habituation across DLPFC subregions showed a reliable difference in p46d. **B**. Ramping activation in TO-number deviants compared to TO-habituation across DLPFC subregions also showed a reliable difference in p46d. **C**. Voxel wise contrasts of ramping activation TO-Rule Deviant > TO-Habituation (Hot colors) false discovery rate (FDR) error cluster corrected for multiple comparisons (FDRc < 0.05, height p < 0.005 unc., extent = 73), overlayed with ramping activation from TO-Habituation > TO-Rule Deviant (Cold colors) false discovery rate (FDR) error cluster corrected for multiple comparisons (FDRc < 0.05, height p < 0.005 unc., extent = 71) are shown. **D**. Voxel wise contrasts of

ramping activation in TO-Number Deviant > TO-Habituation (Hot) false discovery rate (FDR) error cluster corrected for multiple comparisons (FDRc < 0.05, height p < 0.005 unc., extent = 69), overlayed with ramping activation in TO-Habituation > TO-Number Deviant (Cold) false discovery rate (FDR) error cluster corrected for multiple comparisons (FDRc < 0.05, height p < 0.005 unc., extent = 65) are shown. Color bars indicate T-values in **C** and **D**.

Image deviants do not elicit activity in the posterior fundus of area 46

Beyond the change in timing structure, deviants in the SEQ task also contained less frequent, deviant images. It is unlikely that the deviant responses observed in the SEQ task were driven by these images, because deviant comparisons were all made across conditions that contained images from the deviant pool (e.g., SEQ-rule deviant vs. NISR, **Figure 1**). However, infrequent or surprising images have been shown drive responses in LPFC (Chao et al. 2018; Camalier et al. 2019; Grohn et al. 2020). Therefore, we aimed determine if responses in area 46 could be driven by less frequent image presentations, independent of sequential context. To examine this potential functional specificity, we again used conditions that were separate from an abstract visual sequence, i.e., in the TO task. We examined the responses to the randomly interspersed deviant images, hereafter referred to as TO-image deviants and compared them to TO-habituation images to ensure other aspects of the task were held constant.

We found that TO-image deviant responses were not reliably different from TO-habituation image responses in right p46f ($p = 0.67$, **Figure 7A**) or in several of the surrounding subregions: a46d, a46v, p46d (p's > 0.15, **Table 15**). Results from a whole brain contrast comparing TO-image deviants to TO-habituation in the onsets model supported the ROI results (**Figure 7B**,

Table 16). In TO-Image Deviant > TO-Habituation there were no significant clusters in the frontal cortex. However, there were clusters of activation to less frequent stimuli outside the frontal cortex in the cerebellum, thalamus, and across the visual cortex. Thus, although PFC including area 46 did not show increased responses to less frequent or "surprising" stimuli, other areas exhibited such potentially sensory driven responses.

In contrast to right p46f, subregions a46f and p46v differentiated between TO-image deviants and TO-habituation, but with reliably greater responses for habituation images (p's < 0.04, **Figure 7A**). We directly compared responses in p46f to these and other subregions to determine if the response to images (or lack thereof) was regionally specific. In right p46f we found that onset responses to TO-image deviant compared to TO-habituation were reliably different from p46v (ROI x condition: $p < 0.03$) and marginally different from a46f (ROI x condition: $p < 0.11$, **Table 17**). These ROI results showing greater responses to habituation than deviant images were also supported by whole brain contrasts (**Figure 7B**). Significant clusters of activation were observed for TO-Habituation > TO-Image Deviant in right p46v but no other area 46 subregions. Outside of area 46, significant clusters of activation were observed in 44, caudal medial frontal pole, 45a, 45b, superior temporal sulcus, temporal and visual cortices (**Table 16**). We could only speculate on the meaning of greater responses to TO-habituation than TO-image deviants as being potentially related to their previous association with abstract sequences (see Discussion). Regardless, these results highlight the fact that LPFC processes sensory and sequence expectation in different ways, with information about image frequency/expectation primarily localized to p46v and abstract visual sequence processing in p46f.

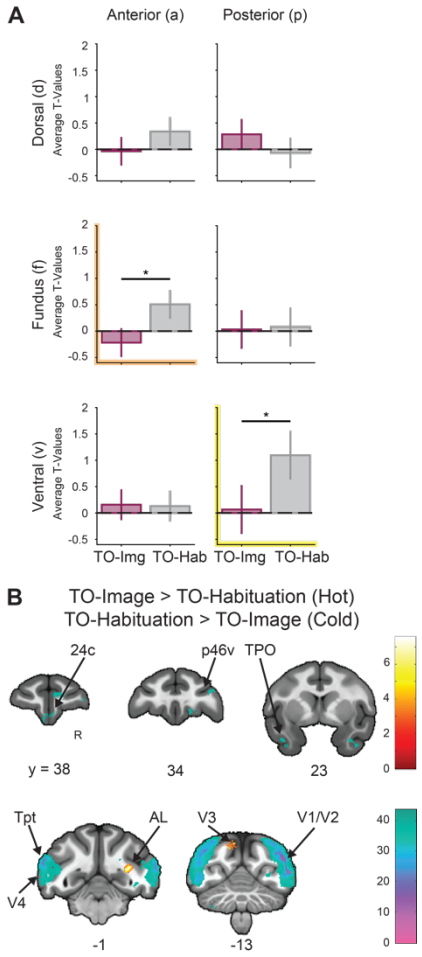

Figure 7. Right p46v and not p46f shows onset responses to image deviants in the TO task. T-values for the condition of interest > baseline are shown. Left column indicates anterior regions and right indicates posterior regions. First row corresponds to dorsal, second to fundus and third to ventral regions. Error bars are 95% confidence intervals (1.96 x standard error of the within-bin mean). Asterisks in graphs indicate significance within comparisons and highlighted axes denote significant interaction of subregion and condition when compared to p46f. **A.** TO-image deviants compared to TO-habituation across DLPFC subregions showing reliable differences in a46f and p46v. Responses in p46f were significantly different from those in p46v and marginally different from those in a46f. **B.** Voxel wise contrasts of TO-Image Deviant > TO-Habituation (Hot) false discovery rate (FDR) error cluster corrected for multiple comparisons (FDRc < 0.05, height p < 0.005 unc., extent = 101), overlaid with TO-Habituation > TO-Image Deviant (Cold) false discovery rate (FDR) error cluster corrected for multiple comparisons (FDRc < 0.05, height p < 0.005 unc., extent = 88) are shown. Color bar indicates T-values.

For completeness, we examined responses in left p46 to determine if TO-image deviants elicited changing in ramping activity. We did not expect changes in ramping to be present because this dynamic has primarily been associated with abstract sequences and timing. Our findings supported this expectation. There were no reliable ramping differences between TO-deviant images and TO-habituation in any subregion of area 46 (**Figure 8A**, **Table 18**). As expected, left p46f ramping responses were also not reliably different from any of the other five subregions (p's > 0.67, **Table 19**). These results were supported by the whole brain contrast (**Figure 8B**) which did not show activation in area 46 but did serve as a positive control and show greater responses to deviant images in cerebellum along with greater responses to habituation images in dorsal area 9, insula, TPO, and visual areas V2 and V3d (**Table 20**). Therefore, image deviant responses are not a likely component of ramping responses to abstract visual sequence responses.

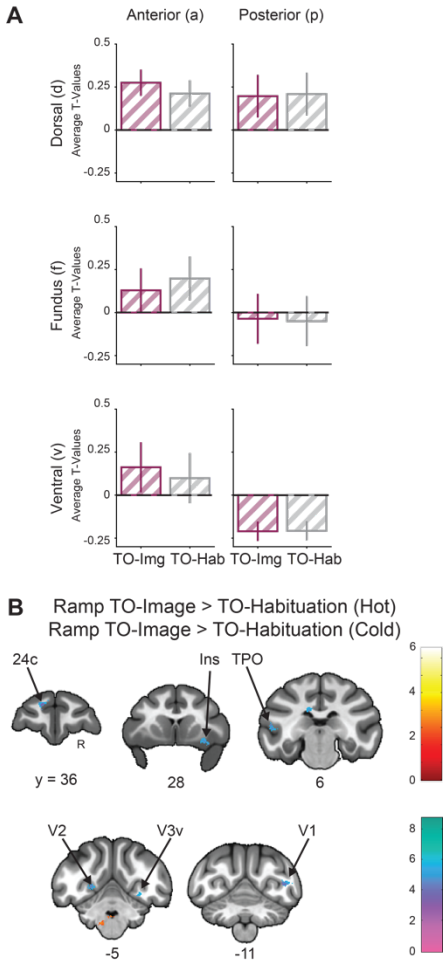

Figure 8. Left p46f does not show ramping responses to image deviants in the TO task. T-values for the condition of interest > baseline are shown. Left column indicates anterior regions and right indicates posterior regions. First row corresponds to dorsal, second to fundus and third to ventral regions. Error bars are 95% confidence intervals (1.96 x standard error of the within-bin mean). **A.** Ramping activation in TO-image deviants compared to TO-habituation across DLPFC subregions showed no significant differences. **B.** Voxel wise contrasts of ramping activity in TO-Image Deviant > TO-Habituation (Hot) false discovery rate (FDR) error cluster corrected for multiple comparisons (FDRc < 0.05, height p < 0.005 unc., extent = 202), overlaid with ramping activation in TO-Habituation > TO-Image Deviant (Cold) false discovery rate (FDR) error cluster corrected for multiple comparisons (FDRc < 0.05, height p < 0.005 unc., extent = 89) are shown. Color bars indicate T-values.

Discussion

We tested the anatomical and functional specificity of abstract visual sequence responses in monkey area 46. In parallel, we aimed to determine the correspondence with human sequence related dynamics, namely ramping. We focused on one particular subregion, the posterior fundus of the principal sulcus (p46f), as it showed the greatest overlap with an ROI where deviant responses have been previously observed in an abstract sequence task (REF NYR). With respect to anatomical specificity, among the six subregions of area 46 (a46d, f, v, and p46d, f, v), only p46f showed significant responses to both rule and number deviants in the abstract visual sequence task (SEQ) with onset dynamics. Similarly, abstract rule deviants elicited significant changes in ramping activation in a distinct cluster of left area 46 that partially overlapped p46f during SEQ, reinforcing parallels to previous results and human abstract sequence responses. The p46f response was also functionally specific to abstract visual sequence deviants. Changes in timing or image alone did not elicit reliable activation in p46f with onset or ramping dynamics. However, other regions, including adjacent regions in area 46, did respond to changes in timing or image alone. Changes in onset activity related to both timing and image were primarily observed in p46v, and to a slightly lesser extent, a46f; whereas changes in time related ramping activity were observed in p46d. Together, these results provide evidence for the anatomical and functional specificity of subregions within area 46, with p46f responding to abstract visual sequence changes and adjacent subregions responding to stimulus changes that could be components of the sequence (time and image). Such specificity further supports the functional

parcellation of area 46 and lays the foundation for a complex and specific functional "map" within DLPFC.

The anatomical specificity of these results aligns with a recent multimodal parcellation of macaque area 46 based on receptor density, cytoarchitectonics, and functional connectivity (Rapan et al. 2023). This parcellation revealed novel subdivisions of area 46 that, strikingly, align with functional responses in this study. Broadly, posterior subregions ('p46') showed more widespread connectivity than anterior subregions ('a46'). Hierarchical clustering, driven by the distribution of receptors, revealed that anterior subregions (a46d, a46f, a46v) along with posterior fundus (p46f) cluster with the most rostral regions of prefrontal cortex. In particular, the fundus regions contained higher levels of norepinephrine alpha-2 receptors, which may be important for regulating persistent neural activity in the region. In contrast, posterior shoulder regions (p46d, p46v) cluster with more caudal premotor areas (and had significantly lower alpha-2 receptor density). Together, these results suggest a unique confluence of properties in p46f such that it is both highly interconnected and shows a broad distribution of receptors, rendering it capable of a variety of response dynamics by integrating information from across the brain. Such interconnectivity may be necessary to integrate information across time such as in the response to abstract visual sequence deviants and is reminiscent of observations in human RLPFC, which is postulated to be the human analog of this region (Sallet et al. 2013).

We did not observe responses in p46f to changes in timing template alone. However, we did observe areas outside p46f that showed such responses. Specifically, within area 46, right p46v showed time deviant responses in onset dynamics, and left p46d showed time deviant responses

in ramping dynamics. These results potentially complement the parcellation findings that the posterior shoulder regions of area 46 cluster with more caudal premotor/sensory processing areas (Rapan et al. 2023). These observations are also generally consistent with previous observations of timing-related activity in monkey LPFC and accompanying dynamics (Niki and Watanabe 1979; Onoe et al. 2001; Genovesio et al. 2006; Cueva et al. 2020; Chiba et al. 2021), although the precise anatomical location was not specified. Human LPFC responses in temporal expectation tasks (Coull and Nobre 2008) were also similar. Outside of area 46 we observed some of the same regions that have been observed for duration perception in monkeys, such as putamen, cerebellum, and V2 (Onoe et al. 2001). We also observed regions similar to those observed in humans related to temporal expectation such as the basal ganglia, temporal cortex, and cerebellum (Coull and Nobre 2008). Together these results illustrate the exquisite specificity of subregions within area 46 and suggest that adjacent subregions code for different stimulus properties (abstract in the fundus and more concrete on the shoulders) that are all important for tracking information through time.

We also did not observe responses in p46f to image deviants alone but did observe responses outside this region. Within area 46, p46v and a46f differentiated between habituation and deviant images. However, responses were greater to habituation images than deviant images, suggesting that this response was not a typical ‘surprise’ response. It is possible that such responses could be partially driven by the fact that there were more habituation than deviant images and thus a greater summed BOLD response. Indeed, the number of images may have been the primary driver in regions such as visual cortex, which showed relatively large areas in TO-Habituation > TO-Image Deviant. However, if frequency was the only driver of such responses then we would

likely observe these responses throughout the whole brain rather than the specific set of regions that were observed. Outside of the visual cortex there were roughly equal numbers of areas that showed responses to the reverse contrast, TO-Image Deviant > TO-Habituation, they were just not located in area 46. An intriguing possibility is that a greater response to the habituation images in area 46 is due to the previous association that those images have to abstract visual sequences, or their greater familiarity (Rainer et al. 1999; Stern et al. 2001; Leaver et al. 2009). Further investigation will be necessary to determine if that is a component of the response in area 46 (a46f and p46v) along with regions observed for TO-Habituation > TO-Image Deviant in the whole brain. There were a small number of regions observed outside of the frontal cortex that showed significantly greater responses to deviant images. These regions were not necessarily overlapping with areas typically associated with 'surprise' or prediction error (Grohn et al. 2020), again raising the prospect that a form of association may govern these responses as well. Further research will be needed to discern the underlying driving forces, but the fact remains that sensory related responses localize to p46v and a46f, and not adjacent p46f, again illustrating the specificity of responses within area 46.

This study's approach was limited in the following ways. First, though individual subregions of area 46 showed significant differences in specific conditions while others did not, the statistical separation from nearby regions was marginal in some cases. This result could be related to limitations of whole-brain event-related monkey fMRI: the spatial resolution, signal-to-noise, and inherent smoothness of the data. Given the size of the subregions (approximately 1.4 cm^3) related to voxel size (1.1 mm^3) there could be differences in alignment of the voxels with the regions and partial volume effects that would be difficult to resolve without fundamentally

changing the experiment by scanning a small volume at higher resolution, using a greater field strength (which may not be available), or greatly increasing the sample size (introducing other limitations). However, these experiments provide an ideal foundation for techniques with higher spatial resolution such as electrophysiological recordings. Other limitations are more general and have been noted in the past (Yusif Rodriguez et al. 2023). Briefly, there were three: it was not possible to examine responses to individual sequence items in a single experiment given the amount of jitter necessary for the BOLD response; the no-report paradigm, while eliminating possible response confounds, did not allow for direct correlations with behavioral performance; and we have focused on a single region, the DLPFC. These limitations again remain important avenues of future research.

In conclusion, we provide unique evidence for the anatomical and functional specificity of abstract visual sequence responses in a specific subregion of LPFC, p46f. These results reinforce the potential parallel with human RLPFC and underscore the importance of the region in tracking abstract information through time. Further, these results highlight the necessity of carefully examining the subregion specificity within LPFC. What may have in the past appeared to be a heterogenous region with respect to specific responses, may in fact contain a more specific set of subdivisions and mapping of function. This study lays the foundation for an approach to functionally dissociating subregions in the cortical structures that underlie many complex and abstract daily functions, such as cooking a meal or appreciating a piece of music.

Tables

Table 1. Data excluded and included for analysis.

Percent Excluded Fixation

	Monkey B	Monkey J	Monkey W
SEQ	6.89%	10.46%	3.03%
Time Only	5.06%	6.96%	10.13%

Percent Excluded Motion

	Monkey B	Monkey J	Monkey W
SEQ	15.15%	0%	0.6%
Time Only	1.89%	16.5%	0.63%

Total Included Runs

	Monkey B	Monkey J	Monkey W	Total Runs
SEQ	70	65	97	232
Time Only	17	38	43	98

Table 2. Regressors used in Onsets and Ramp models. Both tasks are modeled together.

SEQ Regressors	**TO Regressors**
Habituation Block - Habituation Short	Habituation Block - Habituation Short
Habituation Block - Habituation Medium	Habituation Block - Habituation Medium
Habituation Block - Habituation Long	Habituation Block - Habituation Long
Deviant Block - Habituation Short	Deviant Time Block - Habituation Short
Deviant Block - Habituation Medium	Deviant Time Block - Habituation Medium
Deviant Block - Habituation Long	Deviant Time Block - Habituation Long
New Item Same Rule	Deviant Image
Rule Deviant	Rule Deviant Timing
Number Deviant – 2 items	Number Deviant Timing – 2 items
Number Deviant – 6 items	Number Deviant Timing – 6 items
Double Deviant – 2 items	Novel Image Habituation Timing - Short
Double Deviant – 6 items	Novel Image Habituation Timing - Medium
N/A	Novel Image Habituation Timing - Long

Table 3. Onset activity during SEQ-deviants compared to NISR in right area 46 using repeated measures ANOVAs.

P-values in bold are conditions of interest.

SEQ-Rule			Anterior			Posterior		
	Factor	DFs	F	p	eta2p	F	p	eta2p
46d	monkey	2,8	1.8	0.22	0.31	2.8	0.12	0.42
	condition	1,8	0	0.88	0	35.1	**0**	0.81
	monkey:condition	2,8	0.6	0.56	0.13	2.8	0.12	0.41
46f	monkey	2,8	0.3	0.72	0.08	1.2	0.36	0.22
	condition	1,8	0	0.99	0	12.3	**0.01**	0.61
	monkey:condition	2,8	0.7	0.53	0.14	4.6	0.05	0.54
46v	monkey	2,8	0.2	0.8	0.05	4.5	0.05	0.53
	condition	1,8	0.2	0.65	0.03	0	0.93	0
	monkey:condition	2,8	0.7	0.53	0.15	0.2	0.82	0.05
SEQ-Number			Anterior			Posterior		
	Factor	DFs	F	p	eta2p	F	p	eta2p
46d	monkey	2,8	2.1	0.19	0.34	0.5	0.62	0.11
	condition	1,8	8.5	**0.02**	0.52	1.7	0.22	0.18
	monkey:condition	2,8	1.9	0.21	0.32	2.1	0.19	0.34
46f	monkey	2,8	1.1	0.38	0.21	0.6	0.57	0.13
	condition	1,8	0.1	0.73	0.02	5.8	**0.04**	0.42
	monkey:condition	2,8	0.5	0.63	0.11	5.5	0.03	0.58
46v	monkey	2,8	0.1	0.88	0.03	2.8	0.12	0.41
	condition	1,8	0.1	0.79	0.01	0.3	0.58	0.04
	monkey:condition	2,8	0.5	0.6	0.12	0.1	0.88	0.03

Table 4. Coordinates of onset activity clusters in SEQ-rule and SEQ-number deviant > NISR contrasts.

Contrast Location	**Extent (vox)**	**Peak T-val**	**X**	**Y**	**Z**
SEQ-Rule Deviant > NISR					
Rostral Medial Frontal Pole	105	6.25	0.5	45.5	14.5
Dorsal Area 46	381	7.53	14	35.5	25.5
Ventral Area 46	100	5.53	-15	35.5	22
Medial Agranular Insular Region	159	7.53	8	30.5	15
Orbital Area 12	148	5.59	-18	30.5	12.5

Area F5 of Ventral Pre-motor Cortex	173	6.06	-19	13	9.5
Granular Layer of Dentate Gyrus	137	5.66	-9.5	2.5	12.5
Cerebellum	229	4.85	6	-5.5	5.5
Visual Area 2	123	5.65	12	-12	20
	115	7.21	3	-22	23
SEQ-Number Deviant > NISR					
Dorsal Area 46	166	5.73	11	36.5	25.5
Orbital Area 12	133	5.17	-18	31	10.5
Medial Area 13	162	5.21	7.5	27.5	17.5
Visual Area 2	332	7.99	5	-17	18

Table 5. Comparisons of onset activity in right p46f during SEQ-deviants vs. NISR to the five other subregions using repeated measures ANOVAs. P-values in bold are conditions of interest.

SEQ-Rule Comparisons			Anterior			Posterior		
	Factor	DFs	F	p	eta2p	F	p	eta2p
46d	monkey	2,18	1.7	0.2	0.16	3.8	0.04	0.3
	ROI	1,18	1.3	0.28	0.07	0.1	0.76	0.01
	condition	1,18	2.9	0.11	0.14	29	0	0.61
	monkey:condition	2,18	2.8	0.09	0.24	3.8	0.04	0.3
	ROI:condition	1,18	3.9	**0.06**	0.18	0.4	0.53	0.02
46f	monkey	2,18	1.4	0.28	0.13			
	ROI	1,18	0.3	0.57	0.02			
	condition	1,18	1.4	0.24	0.07			
	monkey:condition	2,18	2	0.16	0.18			
	ROI:condition	1,18	1.1	0.31	0.06			
46v	monkey	2,18	0.3	0.72	0.04	0.2	0.82	0.02
	ROI	1,18	0.3	0.62	0.01	5	0.04	0.22
	condition	1,18	1.1	0.32	0.06	2.9	0.11	0.14
	monkey:condition	2,18	2.8	0.09	0.24	1.9	0.17	0.18
	ROI:condition	1,18	3.7	**0.07**	0.17	3.3	**0.09**	0.15
SEQ-Number Comparisons			Anterior			Posterior		
	Factor	DFs	F	p	eta2p	F	p	eta2p
46d	monkey	2,18	0.9	0.42	0.09	1.2	0.33	0.12
	ROI	1,18	0	0.87	0	2	0.18	0.1
	condition	1,18	0.3	0.58	0.02	7	0.02	0.28
	monkey:condition	2,18	6.5	0.01	0.42	6.6	0.01	0.42
	ROI:condition	1,18	15	**0**	0.45	2.3	0.15	0.11
	monkey	2,18	1.1	0.35	0.11			

	ROI	1,18	0	0.94	0			
46f	condition	1,18	1.6	0.22	0.08			
	monkey:condition	2,18	3.9	0.04	0.3			
	ROI:condition	1,18	4.3	**0.05**	0.19			
	monkey	2,18	0.2	0.8	0.02	0.6	0.57	0.06
	ROI	1,18	0.7	0.41	0.04	3.7	0.07	0.17
46v	condition	1,18	3.6	0.07	0.17	1	0.32	0.05
	monkey:condition	2,18	4.7	0.02	0.34	2.5	0.11	0.22
	ROI:condition	1,18	3.7	**0.07**	0.17	6	**0.02**	0.25

Table 6. Ramping activity during SEQ-deviants compared to NISR in left area 46 using repeated measures ANOVAs.

Ramp SEQ-Rule			Anterior			Posterior		
	Factor	DFs	F	p	eta2p	F	p	eta2p
	monkey	2,8	0.1	0.88	0.03	0.4	0.68	0.09
46d	condition	1,8	3.3	0.11	0.29	0.4	0.57	0.04
	monkey:condition	2,8	2.3	0.16	0.37	0.9	0.43	0.19
	monkey	2,8	0.2	0.84	0.04	1.4	0.31	0.26
46f	condition	1,8	1.3	0.29	0.14	2.4	0.16	0.23
	monkey:condition	2,8	0.1	0.93	0.02	0.1	0.89	0.03
	monkey	2,8	0	0.98	0.01	1.4	0.29	0.26
46v	condition	1,8	4.2	0.07	0.34	0.1	0.73	0.02
	monkey:condition	2,8	0	0.99	0	0.5	0.62	0.11
Ramp SEQ-Number			Anterior			Posterior		
	Factor	DFs	F	p	eta2p	F	p	eta2p
	monkey	2,8	0.1	0.95	0.01	0.3	0.74	0.07
46d	condition	1,8	0.6	0.45	0.07	0.2	0.69	0.02
	monkey:condition	2,8	0.4	0.66	0.1	0	0.96	0.01
	monkey	2,8	0.4	0.7	0.08	3.6	0.08	0.48
46f	condition	1,8	1.1	0.32	0.12	1.5	0.26	0.15
	monkey:condition	2,8	0.5	0.65	0.1	0.9	0.44	0.18
	monkey	2,8	0.2	0.81	0.05	0.5	0.65	0.1
46v	condition	1,8	0.1	0.75	0.01	0.2	0.68	0.02
	monkey:condition	2,8	0.1	0.93	0.02	2.4	0.15	0.37

Table 7. Coordinates of ramping activity clusters in SEQ-rule and SEQ-number deviant > NISR contrasts.

Contrast Location	Extent (vox)	Peak T-val	X	Y	Z
Ramp SEQ-Rule Deviant > NISR					
Area 46 Fundus of the Principal Sulcus	98	4.55	-11	34.5	22
Area 24b	95	6.33	0	30.5	25
Lateral Area 13	132	12.48	-15	30	15
Putamen	90	6.84	7.5	26	8
Caudal Dorsal Premotor Cortex	98	6.2	-19	20.5	30
Caudate Nucleus	315	6.23	-10	19.5	23.5
Caudal Dorsal Premotor Cortex	91	8.37	12.5	19	34
Thalamus	90	5.42	-1.5	17.5	15.5
Area IPa	89	6	17	17	1
Internal Capsule	335	12.09	-8.5	13.5	9.5
Granular Insula	89	5.67	18	8.5	16.5
Posterior Dorsal Area TE	134	7.25	27	3	8.5
Caudal Inferior Parietal Lobule Area 7a	93	5.76	17	-1.5	29.5
Visual Area 2	154	9.23	29.5	-7	15.5
Cerebellum	84	5.98	-3.5	-11	9.5
Primary Visual Cortex	136	6.02	25.5	-12	13
Ramp SEQ-Number Deviant > NISR					
Agranular and Dysgranular Insula	85	5.19	21	19.5	11
Thalamus	328	5.42	-3	17	12.5
Anterior Lateral Belt Region	122	7.67	27	16	13.5
Areas 3a and 3b	96	5.38	19	12.5	25.5
Areas 1 and 2	119	5.34	-14	7	34.5
Pons	334	6.88	-4	4.5	2
Cerebellum	105	7.03	7.5	-3.5	-3
Ventral Visual Area 4	78	4.58	15.5	-3.5	10
Visual Area 2	149	5.78	-28	-7.5	18.5
Cerebellum	89	4.86	3.5	-11	6.5
Visual Area 2	91	5.66	-1.5	-12	21.5
Ventral Visual Area 6A	266	6.39	1	-14	26.5
Primary Visual Cortex	74	6.39	-3.5	-22	24

Table 8. Comparisons of ramping activity in left p46f during SEQ-deviants vs. NISR to the five other subregions using repeated measures ANOVAs. P-values in bold are conditions of interest.

Ramp SEQ-Rule Comp.			Anterior			Posterior		
	Factor	DFs	F	p	eta2p	F	p	eta2p
46d	monkey	2,18	1.2	0.33	0.12	0.4	0.7	0.04
	ROI	1,18	7	0.02	0.28	1.7	0.21	0.09
	condition	1,18	0.5	0.5	0.03	0.5	0.51	0.02
	monkey:condition	2,18	0.9	0.44	0.09	0.9	0.42	0.09
	ROI:condition	1,18	6.7	**0.02**	0.27	2	0.18	0.1
46f	monkey	2,18	0.7	0.51	0.07			
	ROI	1,18	1.3	0.27	0.07			
	condition	1,18	0.2	0.65	0.01			
	monkey:condition	2,18	0.2	0.82	0.02			
	ROI:condition	1,18	4.7	**0.04**	0.21			
46v	monkey	2,18	0.8	0.46	0.08	3.1	0.07	0.26
	ROI	1,18	4.9	0.04	0.22	1.5	0.23	0.08
	condition	1,18	0.1	0.77	0.01	0.6	0.45	0.03
	monkey:condition	2,18	0.1	0.94	0.01	0.6	0.56	0.06
	ROI:condition	1,18	7.9	**0.01**	0.3	1.5	0.24	0.08

Ramp SEQ-Number Comp.			Anterior			Posterior		
	Factor	DFs	F	p	eta2p	F	p	eta2p
46d	monkey	2,18	1.6	0.22	0.15	2	0.17	0.18
	ROI	1,18	0.2	0.69	0.01	0	0.97	0
	condition	1,18	2	0.17	0.1	1.3	0.26	0.07
	monkey:condition	2,18	0.3	0.75	0.03	0.5	0.59	0.06
	ROI:condition	1,18	0.1	0.8	0	0.2	0.68	0.01
46f	monkey	2,18	2.1	0.15	0.19			
	ROI	1,18	0.1	0.79	0			
	condition	1,18	0.1	0.79	0			
	monkey:condition	2,18	0.6	0.58	0.06			
	ROI:condition	1,18	1.6	0.22	0.08			
46v	monkey	2,18	1.6	0.23	0.15	2.7	0.1	0.23
	ROI	1,18	1	0.34	0.05	0	0.99	0
	condition	1,18	1.3	0.27	0.07	0.6	0.45	0.03
	monkey:condition	2,18	0.6	0.57	0.06	1	0.38	0.1
	ROI:condition	1,18	0.2	0.68	0.01	0.4	0.53	0.02

Table 9. Onset activity during TO-rule and -number deviants compared to TO-habituation in right area 46 using repeated measures ANOVAs. P-values in bold are conditions of interest.

TO-Rule			Anterior			Posterior		
	Factor	DFs	F	p	eta2p	F	p	eta2p
46d	monkey	2,8	0.1	0.93	0.02	0.3	0.73	0.08
	condition	1,8	7	**0.03**	0.47	0	0.87	0
	monkey:condition	2,8	1	0.41	0.2	1.3	0.33	0.24
46f	monkey	2,8	3.3	0.09	0.45	0.8	0.5	0.16
	condition	1,8	7.4	**0.03**	0.48	0	0.86	0
	monkey:condition	2,8	1	0.42	0.19	0.1	0.95	0.01
46v	monkey	2,8	0.8	0.48	0.17	9.6	0.01	0.71
	condition	1,8	0.2	0.69	0.02	6.8	**0.03**	0.46
	monkey:condition	2,8	0.2	0.79	0.06	5.1	0.04	0.56
TO-Number			Anterior			Posterior		
	Factor	DFs	F	p	eta2p	F	p	eta2p
46d	monkey	2,8	0.1	0.86	0.04	0.3	0.73	0.08
	condition	1,8	2.6	0.15	0.24	0.2	0.7	0.02
	monkey:condition	2,8	0.7	0.55	0.14	0.7	0.51	0.15
46f	monkey	2,8	0.6	0.56	0.13	0.1	0.95	0.01
	condition	1,8	1.7	0.23	0.18	0	0.85	0
	monkey:condition	2,8	1.8	0.23	0.31	1.1	0.37	0.22
46v	monkey	2,8	0.7	0.54	0.14	14.5	0	0.78
	condition	1,8	0.4	0.54	0.05	10	**0.01**	0.55
	monkey:condition	2,8	2.1	0.19	0.34	4.4	0.05	0.52

Table 10. Coordinates of onset activity clusters in TO-rule and TO-number deviant > TO-habituation contrasts.

Contrast Location	**Extent (vox)**	**Peak T-val**	**X**	**Y**	**Z**
TO-Rule Deviant > TO-Habituation					
Putamen	135	6.8	15.5	22.5	10.5
Temporal Parietooccipital Associated Area	113	5.71	-16	22.5	2
Secondary Somatosensory Cortex	92	6.31	25	18	14
Amygdala	85	5.03	8.5	17.5	1.5
Putamen	137	5.33	-15	15.5	13
Areas 1 and 2	84	4.69	-24	12.5	21
Visual Area 2	192	5.77	-12	-5.5	14
Cerebellum	112	6.1	-8	-9.5	10

Visual Area 2	150	5.26	-14	-18	10.5
Primary Visual Cortex	184	6.63	-6	-22	18.5
Primary Visual Cortex	197	5.44	-16	-22	18.5
TO-Habituation > TO-Rule Deviant					
Lateral Area 13	204	6.61	-15	33.5	18
Putamen	227	5.45	12.5	21	19
Area 29	494	7.43	16	0	12
TO-Number Deviant > TO-Habituation					
Dorsal Area 46	142	5.75	-7.5	45	22.5
Intermediate Agranular Insula Area	144	6.37	-11	32	9
Area F5 of Ventral Premotor Cortex	94	7.27	26	27	17.5
Agranular and Dysgranular Insula	177	6.52	21	22	15
Area TEm	222	11	-25	8	7
		3.92	-20	4.5	2
Ventral Intraparietal Area	119	4.76	8.5	5	26
Area Pga	244	6.73	-18	4	16.5
Medial Superior Temporal Area	252	6.09	-14	-1	22
Posterior Intraparietal Area	604	6.9	9.5	-5	22.5
TO-Habituation > TO-Number Deviant					
Area F5 of Ventral Premotor Cortex	123	4.65	-21	29	17.5
Putamen	137	4.57	12	27.5	10.5
Putamen	110	5.16	-17	8.5	12
Temporal Parietooccipital Associated Area	141	6.34	22.5	5	14
Dorsal Visual Area 4	171	7.22	-28	-0.5	17.5
Dorsal Visual Area 4	183	5.95	-28	-4.5	21.5
Lateral Reticular Nucleus	104	4.58	5.5	-7	-4
Primary Visual Cortex	504	6.36	25.5	-7.5	16.5
Primary Visual Cortex	215	5.22	21.5	-12	20.5
Primary Visual Cortex	192	5.29	-20	-13	26

Table 11. Comparisons of onset activity in right p46f during TO-rule and -number deviants vs. TO-habituation to the five other subregions using repeated measures ANOVAs. P-values in bold are conditions of interest.

TO-Rule Comparisons			Anterior			Posterior		
	Factor	DFs	F	p	eta2p	F	p	eta2p
46d	monkey	2,18	0.7	0.52	0.07	0.6	0.54	0.07
	ROI	1,18	0.1	0.74	0.01	0.2	0.64	0.01
	condition	1,18	2.8	0.11	0.14	0	0.97	0
	monkey:condition	2,18	0.2	0.86	0.02	0.5	0.59	0.06
	ROI:condition	1,18	1.3	0.27	0.07	0	0.84	0

	monkey	2,18	3.8	0.04	0.3			
	ROI	1,18	0.7	0.41	0.04			
46f	condition	1,18	3.6	0.08	0.16			
	monkey:condition	2,18	0.2	0.78	0.03			
	ROI:condition	1,18	1.6	0.22	0.08			
	monkey	2,18	1.7	0.21	0.16	6.3	0.01	0.41
	ROI	1,18	0	0.86	0	8.4	**0.01**	0.32
46v	condition	1,18	0.1	0.71	0.01	2.8	0.11	0.14
	monkey:condition	2,18	0.2	0.84	0.02	1.9	0.19	0.17
	ROI:condition	1,18	0	0.94	0	3.1	**0.09**	0.15

TO-Number Comparisons			Anterior			Posterior		
	Factor	DFs	F	p	eta2p	F	p	eta2p
	monkey	2,18	0.1	0.86	0.02	0.1	0.95	0.01
	ROI	1,18	0	0.87	0	0.2	0.69	0.01
46d	condition	1,18	2	0.17	0.1	0	0.88	0
	monkey:condition	2,18	1.8	0.2	0.17	2	0.17	0.18
	ROI:condition	1,18	1.1	0.3	0.06	0.1	0.71	0.01
	monkey	2,18	0.5	0.64	0.05			
	ROI	1,18	0.3	0.56	0.02			
46f	condition	1,18	1.6	0.22	0.08			
	monkey:condition	2,18	2.9	0.08	0.24			
	ROI:condition	1,18	1.1	0.3	0.06			
	monkey	2,18	0.4	0.68	0.04	3.4	0.06	0.27
	ROI	1,18	0	0.91	0	8.2	**0.01**	0.31
46v	condition	1,18	0.4	0.53	0.02	5.3	0.03	0.23
	monkey:condition	2,18	3.4	0.05	0.28	5	0.02	0.36
	ROI:condition	1,18	0.1	0.74	0.01	4.3	**0.05**	0.19

Table 12. Ramping activity during TO-rule and -number deviants compared to TO-habituation in left area 46 using repeated measures ANOVAs. P-values in bold are conditions of interest.

Ramp TO-Rule			Anterior			Posterior		
	Factor	DFs	F	p	eta2p	F	p	eta2p
	monkey	2,8	0.4	0.68	0.09	1.4	0.3	0.26
46d	condition	1,8	0.4	0.55	0.05	7.6	**0.02**	0.49
	monkey:condition	2,8	1.6	0.27	0.28	0.1	0.91	0.02
	monkey	2,8	1	0.4	0.2	0.7	0.53	0.15
46f	condition	1,8	1.6	0.24	0.17	1.6	0.25	0.16
	monkey:condition	2,8	0.3	0.72	0.08	2.3	0.17	0.36
	monkey	2,8	2.8	0.12	0.41	1	0.4	0.2

46v	condition	1,8	2	0.19	0.2	0.4	0.54	0.05
	monkey:condition	2,8	0.6	0.59	0.12	0.1	0.93	0.02

Ramp TO-Number			Anterior			Posterior		
	Factor	DFs	F	p	eta2p	F	p	eta2p
46d	monkey	2,8	3.1	0.1	0.43	0.5	0.62	0.11
	condition	1,8	3.1	0.11	0.28	7.4	**0.03**	0.48
	monkey:condition	2,8	1.8	0.23	0.31	4.5	0.05	0.53
46f	monkey	2,8	0.8	0.49	0.16	2.2	0.17	0.35
	condition	1,8	0.9	0.37	0.1	0	0.88	0
	monkey:condition	2,8	0.7	0.55	0.14	0.8	0.5	0.16
46v	monkey	2,8	4.4	0.05	0.52	2	0.19	0.34
	condition	1,8	2.3	0.17	0.22	0.5	0.49	0.06
	monkey:condition	2,8	2.2	0.18	0.35	0.5	0.64	0.11

Table 13. Coordinates of ramping activity clusters in TO-rule and TO-number deviant > TO-habituation contrasts.

Contrast Location	**Extent (vox)**	**Peak T-val**	**X**	**Y**	**Z**
Ramp TO-Rule Deviant > TO-Habituation					
Caudate Nucleus	241	8.22	-4.5	32	19
Gustatory Cortex	178	7.44	18	27.5	13
Caudate Nucleus	254	5.7	9.5	27.5	21
Caudal Dorsal Premotor Cortex	99	8.16	-11	21.5	25.5
Anterior Lateral Belt Region	83	5.09	-28	12	14
Areas 3a and 3b	145	7.04	-7	5.5	35
Dentate Gyrus	77	5.11	13.5	1.5	9.5
Ventral Visual Area 4	132	4.72	20	0	10.5
Ventral Intraparietal Area	73	4.11	9.5	0	23.5
Cerebellum	279	5.28	-4	-5.5	3
Ramp TO-Habituation > TO-Rule Deviant					
Rostral Medial Frontal Pole	96	6.35	0.5	46	20
Lateral Area 13	95	6.57	12	35	13
Secondary Somatosensory Cortex	170	6.54	-21	25.5	11.5
Temporal Parietooccipital Associated Area	231	9.8	22	18	4
Caudate Nucleus	167	4.99	-7	14	20
Caudal Parabelt Region	109	5.99	29.5	9.5	16
Thalamus	384	6.26	6.5	8	15.5
Pars Reticulata Substantia Nigra	81	5.4	-1.5	7.5	2
Thalamus	96	6.54	-6.5	7	18
Visual areas 4 and 1	200	5.99	24.5	0	14.5
		3.3	16.5	-2.5	15.5

Dorsal Visual Area 4	201	10.38	25	-2.5	21.5
Primary Visual Cortex	71	4.56	-18	-2.5	13
Ventral Visual Area 3	86	5.44	-12	-3	11
Primary Visual Cortex	318	6.35	20	-9.5	18
Cerebellum	81	7.58	11	-12	10
Primary Visual Cortex	226	5.3	-15	-15	18.5
Primary Visual Cortex	123	7.39	21.5	-16	20
Primary Visual Cortex	85	7.57	21	-19	8.5
Primary Visual Cortex	74	8.14	9.5	-23	21
Ramp TO-Number Deviant > TO-Habituation					
Latral Area 12	69	4.65	-21	35	14.5
Area 44	109	5.76	16	30.5	17.5
Secondary Somatosensory Cortex	104	4.31	19	21	19.5
Temporal Parietooccipital Associated Area	135	8.06	23.5	15.5	6.5
Areas 1 and 2	216	7.82	-26	11.5	27.5
Primary Motor Cortex	115	10.82	3	11	32.5
Primary Auditory Cortex	265	6.27	-22	2.5	21.5
Pontine Reticular Nucleus	196	6.18	2.5	1	0
White Matter	89	5.26	9	-2	22
Cerebellum	89	7.92	5	-12	3
Cerebellum	195	10.22	0.5	-16	8
Cerebellum	70	6.71	5.5	-18	9
Primary Visual Cortex	142	5.88	-3.5	-23	24
Ramp TO-Habituation > TO-Number Deviant					
Dorsal Periarcuate Area 8A	133	6.08	-15	29	30.5
STS Part of the Temporal Pole	84	6.9	20	27	-1.5
Hypothalamus	74	4.69	3	22.5	11
Secondary Somatosensory Cortex	74	4.86	-25	14.5	15.5
Hippocampus	167	8.01	11.5	10	2
Thalamus	194	6.36	-7	7.5	15.5
Putamen	434	7.9	16	6	10.5
		4.2	14.5	14	9.5
Area TEO	72	5.51	26.5	6	14.5
Ventral Visual Area 4	129	5.4	15.5	3.5	4
Visual Area 2	84	6.4	21	-4	18.5
Posterior Intraparietal Area	68	6.45	-8.5	-6.5	25.5
Primary Visual Cortex	243	7.58	18	-8	18.5
Cerebellum	73	6.02	15.5	-10	5
Cerebellum	186	5.77	-6	-12	5
Visual Area 2	74	5.7	-13	-13	18.5
Visual Area 2	115	6.22	-15	-13	12.5
Visual Area 2	65	6.3	-5	-15	32.5
Primary Visual Cortex	267	10.07	16.5	-16	17
Visual Area 2	99	5.95	20	-16	11.5

Primary Visual Cortex	70	7.79	7.5	-25	14.5

Table 14. Comparisons of ramping activity in left p46f during TO-rule and -number deviants vs. TO-habituation to the five other subregions using repeated measures ANOVAs.

Ramp TO-Rule Comp.			Anterior			Posterior		
	Factor	DFs	F	p	eta2p	F	p	eta2p
46d	monkey	2,18	0	0.96	0	2	0.16	0.18
	ROI	1,18	2	0.17	0.1	0.4	0.54	0.02
	condition	1,18	1.4	0.25	0.07	6.4	0.02	0.26
	monkey:condition	2,18	0.3	0.75	0.03	0.9	0.41	0.09
	ROI:condition	1,18	0	0.88	0	1.7	0.21	0.09
46f	monkey	2,18	0.1	0.92	0.01			
	ROI	1,18	0.7	0.4	0.04			
	condition	1,18	3.2	0.09	0.15			
	monkey:condition	2,18	1.4	0.28	0.13			
	ROI:condition	1,18	0.3	0.58	0.02			
46v	monkey	2,18	0.7	0.53	0.07	1.9	0.19	0.17
	ROI	1,18	0.1	0.71	0.01	1.1	0.3	0.06
	condition	1,18	3.2	0.09	0.15	1.8	0.2	0.09
	monkey:condition	2,18	0.7	0.5	0.07	1.4	0.26	0.14
	ROI:condition	1,18	0.4	0.51	0.02	0	0.98	0

Ramp TO-Number Comp.			Anterior			Posterior		
	Factor	DFs	F	p	eta2p	F	p	eta2p
46d	monkey	2,18	0.3	0.71	0.04	2.3	0.13	0.21
	ROI	1,18	0.3	0.58	0.02	0.3	0.61	0.02
	condition	1,18	1.5	0.24	0.08	2.3	0.14	0.12
	monkey:condition	2,18	1.5	0.24	0.14	2.9	0.08	0.24
	ROI:condition	1,18	1.6	0.23	0.08	1.8	0.2	0.09
46f	monkey	2,18	0.2	0.83	0.02			
	ROI	1,18	0.4	0.52	0.02			
	condition	1,18	0.7	0.42	0.04			
	monkey:condition	2,18	1.3	0.3	0.13			
	ROI:condition	1,18	0.6	0.46	0.03			
46v	monkey	2,18	0.1	0.89	0.01	4.8	0.02	0.35
	ROI	1,18	0	0.84	0	0.4	0.55	0.02
	condition	1,18	1.6	0.22	0.08	0.2	0.68	0.01
	monkey:condition	2,18	2.4	0.12	0.21	0.9	0.41	0.09
	ROI:condition	1,18	1.1	0.32	0.06	0.2	0.63	0.01

Table 15. Onset activity during TO-image deviants compared to TO-habituation in right area 46 using repeated measures ANOVAs. P-values in bold are conditions of interest.

TO-Image			Anterior			Posterior		
	Factor	DFs	F	p	eta2p	F	p	eta2p
46d	monkey	2,8	1	0.42	0.2	0.2	0.82	0.05
	condition	1,8	1	0.35	0.11	2.6	0.15	0.24
	monkey:condition	2,8	0.2	0.81	0.05	1.7	0.24	0.3
46f	monkey	2,8	2.6	0.13	0.39	1.3	0.32	0.25
	condition	1,8	5.8	**0.04**	0.42	0.2	0.67	0.02
	monkey:condition	2,8	0.5	0.61	0.12	3.3	0.09	0.45
46v	monkey	2,8	3.4	0.09	0.46	9.7	0.01	0.71
	condition	1,8	0.1	0.72	0.02	11.8	**0.01**	0.6
	monkey:condition	2,8	0.4	0.7	0.09	10.2	0.01	0.72

Table 16. Coordinates of onset activity clusters in TO-Image Deviant > TO-Habituation and TO-Habituation > TO-Image Deviant contrasts.

Contrast Location	**Extent (vox)**	**Peak T-val**	**X**	**Y**	**Z**
TO-Image Deviant > TO-Habituation					
Hypothalamus	139	5.12	2	15.5	8.5
Middle Temporal Area	374	7.21	10	3	18
		4.83	17	-2.5	20.5
Ventral Visual Area 4	134	7.09	20	-7.5	8.5
Ventral Visual Area 6A	172	5.83	-3	-14	32
Visual Area 2	101	6.3	-7.5	-15	16.5
		4.06	-3	-20	12
TO-Habituation > TO-Image Deviant					
Caudal Medial Frontal Pole	302	5.93	0	40	10.5
Dorsal Area 46	294	6.05	7	37.5	19
		4.84	7.5	45.5	21.5
Medial Area 13	217	7.08	6.5	34.5	12.5
Ventral Area 46	268	6.27	17.5	34.5	23.5
Area 45b	105	4.08	-20	29	22
Area F5 of Ventral Premotor Cortex	146	5.82	22	27.5	12
STS Part of Temporal Pole	339	5.97	15	24.5	-1.5

		3.25	18	17	-3
Anterior Ventral Area TE	472	7.53	-19	21	-2.5
Putamen	568	6.67	13	19	17
		3.41	8	14.5	21.5
Caudal Dorsal Premotor Cortex	187	6.79	17.5	18	31
Area TEm	344	6.17	23.5	9	9
		5.39	18	11.5	3.5
Temporal Parietooccipital Associated Area	171	5.01	-25	5.5	15.5
Medial Pulvinar Nucleus	93	5.09	-5.5	4.5	17.5
Primary Motor Cortex	88	5.35	11	1.5	31
Ventral Visual Area 4	304	5.32	18.5	-0.5	12
Posterior Intraparietal Areas	150	5.39	-11	-4.5	20.5
Visual Area 2	25046	43.43	19	-11	24
		30.66	23.5	-14	17.5
		21.88	28	0.5	21
		17.48	15.5	-15	30.5
		16.25	25	-5	14
		11.1	25.5	-6	25
		10.18	28	3	13
		8.78	11.5	-3	22.5
		6.57	16.5	-19	12.5
		6.35	18.5	-19	22.5
		5.11	13	-13	16.5
		4.97	3.5	-4.5	24
		4.51	16	-5	15.5
		4.16	26.5	6.5	5.5
Visual Area 2	21128	33.77	-20	-11	30
		24.6	-26	-4	20.5
		18.87	-21	-8.5	14
		17.13	-20	-15	21.5
		14.89	-13	-14	32.5
		6.23	-29	0.5	13.5
		6.15	-20	-20	12.5
		4.56	-14	-19	25.5
Cerebellum	205	5.82	-13	-11	-1.5

Table 17. Comparisons of onset activity in right p46f during TO-image deviants vs. TO-habituation to the five other subregions using repeated measures ANOVAs. P-values in bold are conditions of interest.

TO-Image Comparisons	Anterior	Posterior

	Factor	DFs	F	p	eta2p	F	p	eta2p
46d	monkey	2,18	0	0.97	0	1.3	0.3	0.13
	ROI	1,18	0.2	0.63	0.01	0.1	0.76	0.01
	condition	1,18	0.9	0.35	0.05	0.5	0.48	0.03
	monkey:condition	2,18	1.5	0.24	0.14	4.2	0.03	0.32
	ROI:condition	1,18	0.6	0.46	0.03	1	0.32	0.05
46f	monkey	2,18	0.2	0.81	0.02			
	ROI	1,18	0.2	0.68	0.01			
	condition	1,18	4	0.06	0.18			
	monkey:condition	2,18	3.3	0.06	0.27			
	ROI:condition	1,18	2.9	**0.11**	0.14			
46v	monkey	2,18	0	1	0	1.8	0.2	0.17
	ROI	1,18	0.3	0.59	0.02	8.7	0.01	0.33
	condition	1,18	0	0.97	0	7	0.02	0.28
	monkey:condition	2,18	1.8	0.2	0.16	12	0	0.57
	ROI:condition	1,18	0	0.87	0	6	**0.03**	0.25

Table 18. Ramping activity during TO-image deviants compared to TO-habituation in left area 46 using repeated measures ANOVAs. There were no significant differences in any of the subregions.

Ramp TO-Image			Anterior			Posterior		
	Factor	DFs	F	p	eta2p	F	p	eta2p
46d	monkey	2,8	1.9	0.2	0.33	0.9	0.44	0.19
	condition	1,8	0.5	0.49	0.06	0.1	0.77	0.01
	monkey:condition	2,8	0	0.98	0.01	0.3	0.72	0.08
46f	monkey	2,8	0.3	0.73	0.08	3	0.11	0.43
	condition	1,8	0.3	0.61	0.03	0	0.91	0
	monkey:condition	2,8	0.5	0.6	0.12	0.3	0.77	0.06
46v	monkey	2,8	1.2	0.35	0.23	0.9	0.46	0.18
	condition	1,8	0	0.91	0	0.1	0.79	0.01
	monkey:condition	2,8	1.8	0.22	0.31	0.4	0.65	0.1

Table 19. Comparisons of ramping activity in left p46f during TO-image deviants vs. TO-habituation to the five other subregions using repeated measures ANOVAs. There were no significant differences in any of the subregions.

Ramp TO-Image Comp.	Anterior	Posterior

	Factor	DFs	F	p	eta2p	F	p	eta2p
46d	monkey	2,18	0.1	0.88	0.01	2.5	0.11	0.21
	ROI	1,18	1.9	0.19	0.1	1.6	0.22	0.08
	condition	1,18	0.1	0.8	0	0.1	0.78	0
	monkey:condition	2,18	0.3	0.76	0.03	0.3	0.74	0.03
	ROI:condition	1,18	0.1	0.77	0	0	0.89	0
46f	monkey	2,18	0.3	0.75	0.03			
	ROI	1,18	0.8	0.37	0.05			
	condition	1,18	0.2	0.65	0.01			
	monkey:condition	2,18	0.8	0.48	0.08			
	ROI:condition	1,18	0.2	0.67	0.01			
46v	monkey	2,18	0.3	0.72	0.04	3.6	0.05	0.29
	ROI	1,18	0.7	0.43	0.04	0.9	0.36	0.05
	condition	1,18	0	0.99	0	0	0.84	0
	monkey:condition	2,18	1.7	0.2	0.16	0.6	0.58	0.06
	ROI:condition	1,18	0.1	0.8	0	0	0.92	0

Table 20. Coordinates of ramping activity clusters in TO-image deviant > TO-habituation contrasts.

Contrast Location	Extent (vox)	Peak T-val	X	Y	Z
Ramp TO-Image Deviant > TO-Habituation					
Cerebellum	202	6.18	0	-8.5	0
Ramp TO-Habituation > TO-Image Deviant					
Dorsal Area 8B	160	6.47	-3.5	35.5	28.5
Intermediate Agranular Insula Area	131	5.65	12.5	29.5	10
Temporal Parietooccipital Associated Area	163	6.11	-25	6.5	15.5
Area 29	144	5.4	-6	5	23.5
Thalamus	89	4.28	-14	4.5	13.5
Pulvinar	173	5	12	3	19.5
Ventral Visual Area 3	241	5.13	14	-2.5	10
Visual Area 2	113	5.71	-11	-6	16
	234	7.72	21	-9.5	18.5
Cerebellum	91	6.75	5.5	-15	-1.5

References

Ahuja A, Yusif Rodriguez N. 2022. Is the Dorsolateral Prefrontal Cortex Actually Several Different Brain Areas? J Neurosci. 42:6310–6312.

Balan PF, Zhu Q, Li X, Niu M, Rapan L, Funck T, Wang H, Bakker R, Palomero-Gallagher N, Vanduffel W. 2024. MEBRAINS 1.0: A new population-based macaque atlas. Imaging Neuroscience. 2:1–26.

Camalier CR, Scarim K, Mishkin M, Averbeck BB. 2019. A Comparison of Auditory Oddball Responses in Dorsolateral Prefrontal Cortex, Basolateral Amygdala, and Auditory Cortex of Macaque. Journal of Cognitive Neuroscience. 31:1054–1064.

Chao ZC, Takaura K, Wang L, Fujii N, Dehaene S. 2018. Large-Scale Cortical Networks for Hierarchical Prediction and Prediction Error in the Primate Brain. Neuron. 100:1252-1266.e3.

Chiba A, Morita K, Oshio K, Inase M. 2021. Neuronal activity in the monkey prefrontal cortex during a duration discrimination task with visual and auditory cues. Sci Rep. 11:17520.

Coull JT, Nobre AC. 2008. Dissociating explicit timing from temporal expectation with fMRI. Current Opinion in Neurobiology. 18:137–144.

Cueva CJ, Saez A, Marcos E, Genovesio A, Jazayeri M, Romo R, Salzman CD, Shadlen MN, Fusi S. 2020. Low-dimensional dynamics for working memory and time encoding. Proc Natl Acad Sci USA.

Desrochers TM, Chatham CH, Badre D. 2015. The necessity of rostrolateral prefrontal cortex for higher-level sequential behavior. Neuron. 87:1357–1368.

Desrochers TM, Collins AGE, Badre D. 2019. Sequential Control Underlies Robust Ramping Dynamics in the Rostrolateral Prefrontal Cortex. The Journal of Neuroscience. 39:1471–1483.

Genovesio A, Tsujimoto S, Wise SP. 2006. Neuronal Activity Related to Elapsed Time in Prefrontal Cortex. Journal of Neurophysiology. 95:3281–3285.

Grohn J, Schüffelgen U, Neubert F-X, Bongioanni A, Verhagen L, Sallet J, Kolling N, Rushworth MFS. 2020. Multiple systems in macaques for tracking prediction errors and other types of surprise. PLoS Biol. 18:e3000899.

Jung J, Lambon Ralph MA, Jackson RL. 2022. Subregions of DLPFC Display Graded yet Distinct Structural and Functional Connectivity. J Neurosci. 42:3241–3252.

Kim HF, Hikosaka O. 2013. Distinct basal ganglia circuits controlling behaviors guided by flexible and stable values. Neuron. 79:1001–1010.

Leaver AM, Lare JV, Zielinski B, Halpern AR, Rauschecker JP. 2009. Brain Activation during Anticipation of Sound Sequences. J Neurosci. 29:2477–2485.

Leite FP, Tsao D, Vanduffel W, Fize D, Sasaki Y, Wald LL, Dale AM, Kwong KK, Orban G a, Rosen BR, Tootell RBH, Mandeville JB. 2002. Repeated fMRI using iron oxide contrast agent in awake, behaving macaques at 3 Tesla. NeuroImage. 16:283–294.

McKim TH, Desrochers TM. 2022. Reward Value Enhances Sequence Monitoring Ramping Dynamics as Ending Rewards Approach in the Rostrolateral Prefrontal Cortex. eNeuro. 9:ENEURO.0003-22.2022.

Miyashita Y, Higuchi SI, Sakai K, Masui N. 1991. Generation of fractal patterns for probing the visual memory. Neuroscience Research. 12:307–311.

Niki H, Watanabe M. 1979. Prefrontal and cingulate unit activity during timing behavior in the monkey. Brain Res. 171:213–224.

Onoe H, Komori M, Onoe K, Takechi H, Tsukada H, Watanabe Y. 2001. Cortical Networks Recruited for Time Perception: A Monkey Positron Emission Tomography (PET) Study. NeuroImage. 13:37–45.

Petrides M. 2005. Lateral prefrontal cortex: architectonic and functional organization. Philosophical Transactions of the Royal Society B: Biological Sciences. 360:781–795.

Petrides M, Pandya DN. 1984. Projections to the frontal cortex from the posterior parietal region in the rhesus monkey. Journal of Comparative Neurology. 228:105–116.

Petrides M, Pandya DN. 1999. Dorsolateral prefrontal cortex: comparative cytoarchitectonic analysis in the human and the macaque brain and corticocortical connection patterns. European Journal of Neuroscience. 11:1011–1036.

Petrides M, Pandya DN. 2002. Comparative cytoarchitectonic analysis of the human and the macaque ventrolateral prefrontal cortex and corticocortical connection patterns in the monkey. European Journal of Neuroscience. 16:291–310.

Petrides M, Tomaiuolo F, Yeterian EH, Pandya DN. 2012. The prefrontal cortex: Comparative architectonic organization in the human and the macaque monkey brains. Cortex, Frontal lobes. 48:46–57.

Rainer G, Rao SC, Miller EK. 1999. Prospective Coding for Objects in Primate Prefrontal Cortex. J Neurosci. 19:5493–5505.

Rapan L, Froudist-Walsh S, Niu M, Xu T, Zhao L, Funck T, Wang X-J, Amunts K, Palomero-Gallagher N. 2023. Cytoarchitectonic, receptor distribution and functional connectivity analyses of the macaque frontal lobe. eLife. 12:e82850.

Saleem KS, Miller B, Price JL. 2014. Subdivisions and connectional networks of the lateral prefrontal cortex in the macaque monkey. The Journal of comparative neurology. 522:1641–1690.

Sallet J, Mars RB, Noonan MP, Neubert F-X, Jbabdi S, O'Reilly JX, Filippini N, Thomas AG, Rushworth MF. 2013. The organization of dorsal frontal cortex in humans and macaques. J Neurosci. 33:12255–12274.

Sirmpilatze N, Klink PC. 2020. RheMAP: Non-linear warps between common rhesus macaque brain templates.

Stern CE, Sherman SJ, Kirchhoff BA, Hasselmo ME. 2001. Medial temporal and prefrontal contributions to working memory tasks with novel and familiar stimuli. Hippocampus. 11:337–346.

Tanji J, Hoshi E. 2008. Role of the Lateral Prefrontal Cortex in Executive Behavioral Control. Physiological Reviews. 88:37–57.

Walker AE. 1940. A cytoarchitectural study of the prefrontal area of the macaque monkey. Journal of Comparative Neurology. 73:59–86.

Wang L, Uhrig L, Jarraya B, Dehaene S. 2015. Representation of numerical and sequential patterns in macaque and human brains. Current Biology. 25:1966–1974.

Xu R, Bichot NP, Takahashi A, Desimone R. 2022. The cortical connectome of primate lateral prefrontal cortex. Neuron. 110:312-327.e7.

Yusif Rodriguez N, McKim TH, Basu D, Ahuja A, Desrochers TM. 2023. Monkey Dorsolateral Prefrontal Cortex Represents Abstract Visual Sequences during a No-Report Task. J Neurosci. 43:2741–2755.